DEVELOPMENT OF THREE PHASE UNIVERSAL PFC CIRCUIT FOR DC MICROGRID APPLICATION

A DISSERTATION

Submitted in partial fulfillment of the
requirements for the award of the degree
of
INTEGRATED DUAL DEGREE
in
ELECTRICAL ENGINEERING
(With Specialization in Power Electronics)

By

KRITGYA BAWAL

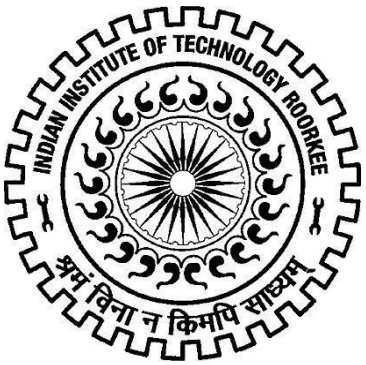

DEPARTMENT OF ELECTRICAL ENGINEERING
INDIAN INSTITUTE OF TECHNOLOGY ROORKEE
ROORKEE -247667 (INDIA)
2016

© INDIAN INSTITUTE OF TECHNOLOGY ROORKEE, 2016

ALL RIGHTS RESERVED

CANDIDATE'S DECLARATION

I hereby declare that the work carried out in this dissertation entitled "**DEVELOPMENT OF THREE PHASE UNIVERSAL PFC CIRCUIT FOR DC MICROGRID APPLICATION**" is presented for partial fulfillment of the requirement for the award of the degree of Integrated Dual Degree with specialization in Power Electronics submitted to the department of Electrical Engineering, Indian Institute of Technology Roorkee, India, under the supervision and guidance of Dr. Avik Bhattacharya, Associate Professor, IIT Roorkee, India.

I have not submitted the matter embodied in this report for the award of any other degree or diploma.

Date:

Place: Roorkee (KRITGYA BAWAL)

CERTIFICATE

This is to certify that the above statement made by the candidate is correct to the best of my knowledge and belief.

(Dr. Avik Bhattacharya)
Assistant Professor,
Department of Electrical Engineering,
Indian Institute of Technology Roorkee
Roorkee-247667, India

ABSTRACT

The present power system is established on the principle of alternating power but there has been an increase in DC loads due to on-going revolution in electronics industry. A solution to eliminate multiple rectification processes is DC micorgrid. AC power converts to DC when entering the DC micro-grid using a high-efficiency rectifier. The DC microgrid considered in the project includes Photovoltaic system, Battery storage and AC grid connected bidirectional rectifier. The topology used for rectifier operation is a three phase two-stage design, with a boost rectifier providing power factor correction at the input to the first stage and a bidirectional dc-dc converter assembling the second stage providing power management for DC microgrid. The bidirectional converter is capable of handling the power flow to load in the condition of mismatch between power generated from PV system and the power required from the load. To validate the operation characteristics the system is extensively simulated in MATLAB/Simulink.

ACKNOWLEDGEMENTS

I wish to affirm my deep sense of gratitude and sincere thanks to my guide Dr. Avik Bhattacharya, Assistant Professor, Department of Electrical Engineering IIT Roorkee, for intuitive and meticulous guidance in completion of this report. I would like to thank them for provision of expertise, and technical support in the implementation, without their guidance and motivation I could not have successfully completed this dissertation.

I would also like to thank Dr. S.P. Srivastava, HoD EED, IIT Roorkee for his constant support. Also I would like to thank all the teaching and non-teaching staff of the department who have contributed directly or indirectly in successful completion of my dissertation work.

I also acknowledge the blessings of my parents for encouragement and moral support rendered to me throughout my life. I also like to thank all of the staffs of Dept. of Electrical Engineering for their support.

Kritgya Bawal

(IDD Electrical, Enrollment No – 11212008)

CONTENTS

LIST OF FIGURES

LIST OF TABLES

LIST OF ACRONYMS

MG	Microgrids
DC	Direct Current
AC	Alternating Current
PFC	Power Factor Correction
THD	Total Harmonics Distortion
PWM	Pulse Width Modulation
PI	Proportional and Integral
IGBT	Insulated Gate Bipolar Transistor
MOSFET	Metal Oxide Semiconductor Field Effect Transistor
PV	Photovoltaic
FFT	Fast Fourier Transform

LIST OF SYMBOLS

V_{ll}	3-Phase line-line rms voltage
V_{out}	Output DC Voltage of boost active rectifier
V_{Bus}	DC microgrid bus Voltage
L	Boost inductor in boost active rectifier
C	Capacitance in boost active rectifier
R	Resistor in boost active rectifier
$L_{b\text{-}b}$	Inductor in Bidirectional DC-DC Converter
I_{pv}	Photocurrent
I_{sat}	Module reverse saturation current
q	Electron charge
A	Ideality factor
k	Boltzman constant
R_s	Series resistance of a PV cell
R_p	Parallel resistance of a PV cell
I_{sso}	Short-circuit current
k_i	SC current temperature coefficient
T_r	Reference temperature
L_{rr}	Reverse saturation current at Tr
E_{gap}	Energy of the band gap for silicon
n_p	Number of cells in parallel
n_s	Number of cells in series
S	Solar radiation level
T_1	Surface temperature of the PV
f_{SB}	Switching frequency of bidirectional DC-DC Converter
L_b	Inductor in MPPT controlled boost converter
C_o	Capacitance in MPPT controlled boost converter
P_{Load}	Power consumed at load
P_{Solar}	Power generated by PV system
P_{grid}	Power supplied from utility grid

CHAPTER 1: INTRODUCTION

1.1 General

The increasing demand of electricity and the environmental concerns introduced a new trend of generating small scale power locally. These days, interests in small scale power generation from the renewable energy resources like photovoltaic and wind power is increasing because they are abundant in nature and environmental friendly. Microgrid (MG) is defined as cluster of distribution generation (DG) sources, distributed storage devices and distributed loads that operate in a controlled manner so as to improve the reliability and quality of the local power supply and of the power system. The different types of existing microgrid are proposed already, as AC or DC micro-grid based on whether the distributed sources and loads connected to AC or DC grid. AC microgrids have advantage of utilizing the existing AC grid network, protection and standards, but synchronization, stability, need for reactive are some of the major challenges existing in AC microgrids. Whereas if the energy from distributed generation utilized in DC form and properly controlled, it would improve the efficiency of the system and also the loss in the power system would be decreased. In addition DC-microgrid enables easier integration to other DC distributed energy resources like photovoltaic, fuel cell and energy storage by power electronic interfaces [1]-[2].

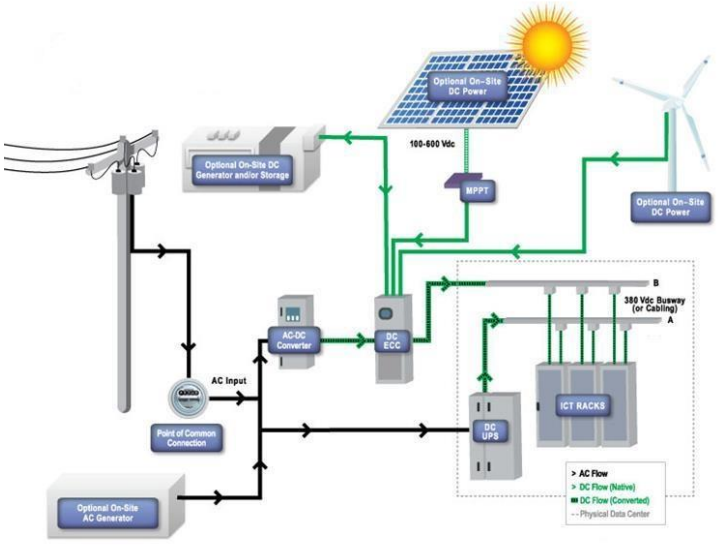

Figure 1.1: A DC microgrid conceptualization

In the DC micro-grid system, AC power converts to DC when entering the DC grid using a high-efficiency rectifier, which then distributes the power directly to DC equipment served by the DC grid. Conventionally, the diode bridge or the thyristor bridge has been the most commonly used AC-DC power converter for obtaining DC power from the AC grid. The use of these bridge topologies is mainly motivated due to their advantage in size, control, reliability, structural simplicity and economics. However, usage of such bridge circuits is quite disadvantageous from the viewpoint of the AC grid, as they inject unwanted current harmonics of relatively high amplitudes (depending on the power level of the bridge) into the grid. Consequently this results in the distortion of the grid voltage, which can cause undesirable disturbances and hence poor power quality in the neighbouring loads connected to the grid. In view of limiting this utility pollution due to power converters, standards (IEEE 519,IEC 61000-3-6)[3] have been introduced which limits the direct use of diode and thyristor bridges, with more emphasis being laid on the use of power converters which have lesser harmonic influence on the grid. Also bidirectional power processing is preferred in the DC microgrid application which requires investigation of improved power quality converters.

1.2 Literature review

This section presents a review of research works that have already been done so far in the field of design and control of three phase ac-dc converters and DC microgrid.

1.2.1 Review based on design and control of three phase ac-dc converters.

A forced commutated ac-dc converter and its control strategy was proposed by *Eugenio Wernekinck* et al. (1987) for unity power factor in three phase system. By the use of improved firing angle current harmonic distortion was diminished for the converter. Only the DC voltage was sensed in the topology and power factor was controlled by relative position of fundamental component of PWM type voltage[4].

Juan W. Dixon (1990) analysed three different control strategies for boost type PWM rectifiers for stability boundaries and complexity of each topology. Accordingly, concluded the direct current control method with hysteresis band as most reliable strategy, because of constant power factor operation and good stability[5].

Rusong Wu (1991) presented a comprehensive analysis of PWM ac-dc voltage source converter and established a general mathematical model of the converter. By use of fourier analysis and reference frame transformation three models steady state dc model, low frequency and high frequency ac models were developed[6].

Marian P., Kazmierkowski & Luigi Malesani (1998) described current control techniques for three phase voltage source pulse width modulated converters in two groups- linear and non linear. Proportional integral and state feedback controllers and predictive with techniques constant switching frequency were included in first group and hysteresis, delta modulation controllers were in second group[7].

A three phase PWM buck-boost rectifier was investigated by *Jun Kikuchi* (2002) taking Cuk-Cuk realization. The operating principle, modulation scheme, steady state and dynamic analyses were discussed. Results demonstrated step-up, step-down, bidirectional power processing and unity power factor operation capabilities of presented three phase PWM buck-boost converter[8].

1.2.2 Review based on configuration and control of DC microgrid

An approach was made by *Robert H. Lasseter & Paolo Paigi* (2004) considering the emerging potential of distributed generation. The proposed microgrid system has ability of island generation and high reliability than the power system as whole[9].

Baochao Wang (2012) proposed a DC microgrid with multilayer control and smart grid communications. The control strategy was concerned on power balancing and imposed power limits by utility grid. Energy management scheme for multi-source power subsystem was described in a multilayer manner[10].

1.3 Organization of the thesis

The thesis consists of six chapters and each chapter discusses a particular aspect of three phase power factor correction circuit for DC microgrid application.

Chapter 1 deals with the introduction, literature review and chapter wise organization of the thesis.

Chapter 2 discusses basic functionality and control strategies for three phase six switch boost converter topology. The calculations for boost inductor design and dc link capacitor design are also discussed.

Chapter 3 proposes a DC microgrid configuration consisting Photovoltaic generation system, energy storage elements, DC loads and utility grid connected bidirectional ac-dc converter. The components of DC microgrid structure are briefly explained and power flow between the components is also covered.

Chapter 4 presents the MATLAB simulation results for three phase six switch boost converter and it's application with bidirectional DC-DC converter in DC microgrid. The bidirectional ac-dc PFC converter was investigated for different cases of DC microgrid.

Chapter 5 discusses the development hardware prototype for three phase six switch boost converter and auxiliary hardware circuits.

Chapter 6 concludes the dissertation thesis and suggests some recommendation for future work.

CHAPTER 2: THREE PHASE SIX-SWITCH BOOST RECTIFIER

Three phase boost power factor correction rectifier has been a preferred solution over wide range of applications due to inherent power quality improvement at input and output with high power density and efficiency. The described topology is capable of bidirectional power processing. Hence, it can operate as a rectifier as well as an inverter. During the rectifier operation the DC link capacitor maintains the output DC voltage V_O and is discharged to feed the DC load. The DC current I_L is positive during the operation and the control structure maintains the power factor near 1. During the inversion the DC current I_L is negative and switching of IGBTs are modified by the control structure in such an order that power factor is close to -1.

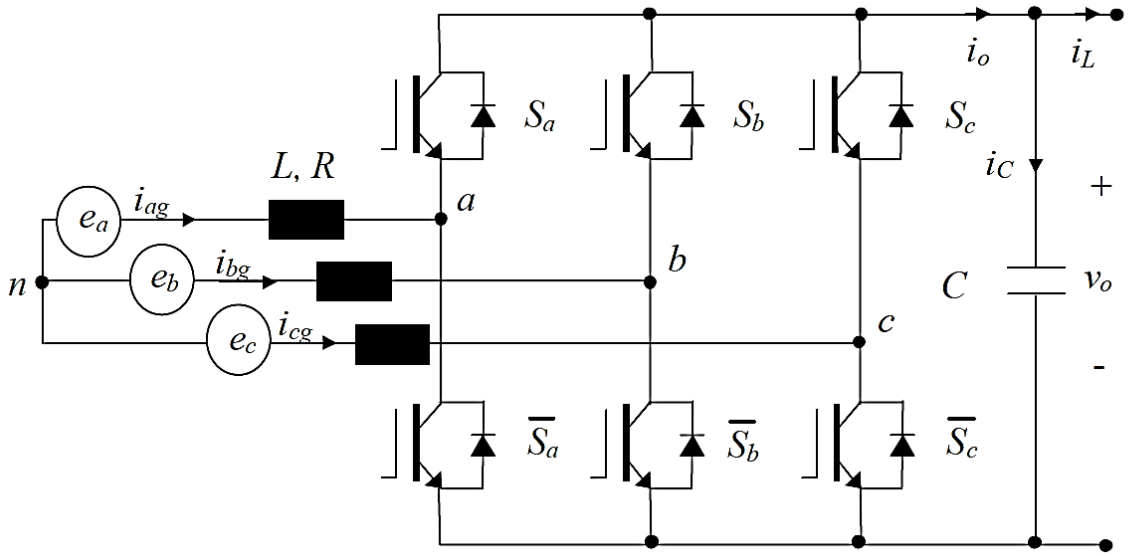

Figure 2.1: Three-phase six-switch two level boost converter topology[11];

There are two control loops which constitute the control structure of three phase boost rectifier i. e. one outer voltage control loop and one inner current control loop. The voltage controller senses the output DC voltage V_O and compare it to the reference voltage V_{ref}. The error signal is processed by PI controller and the resultant signal is used in acquiring reference currents for the inner current controller. The phase information of the utility voltage and current is required for the control of boost rectifier.

2.1 Basic Functioning of boost rectifier

Fig. 2.2 shown below explains the rectification mode of the topology. In Fig. 2.2(a) the lower switch S_4 of first leg (phase 'a') is turned on. The current in phase 'a' is positive and the input source is supplying energy to the inductor. Then upper switch S_1 of the first leg is turned on as shown in Fig 2.2(b). During this period, the output DC side gets energy from the input source as well as the inductor. In result, stepping up the output DC voltage V_O.

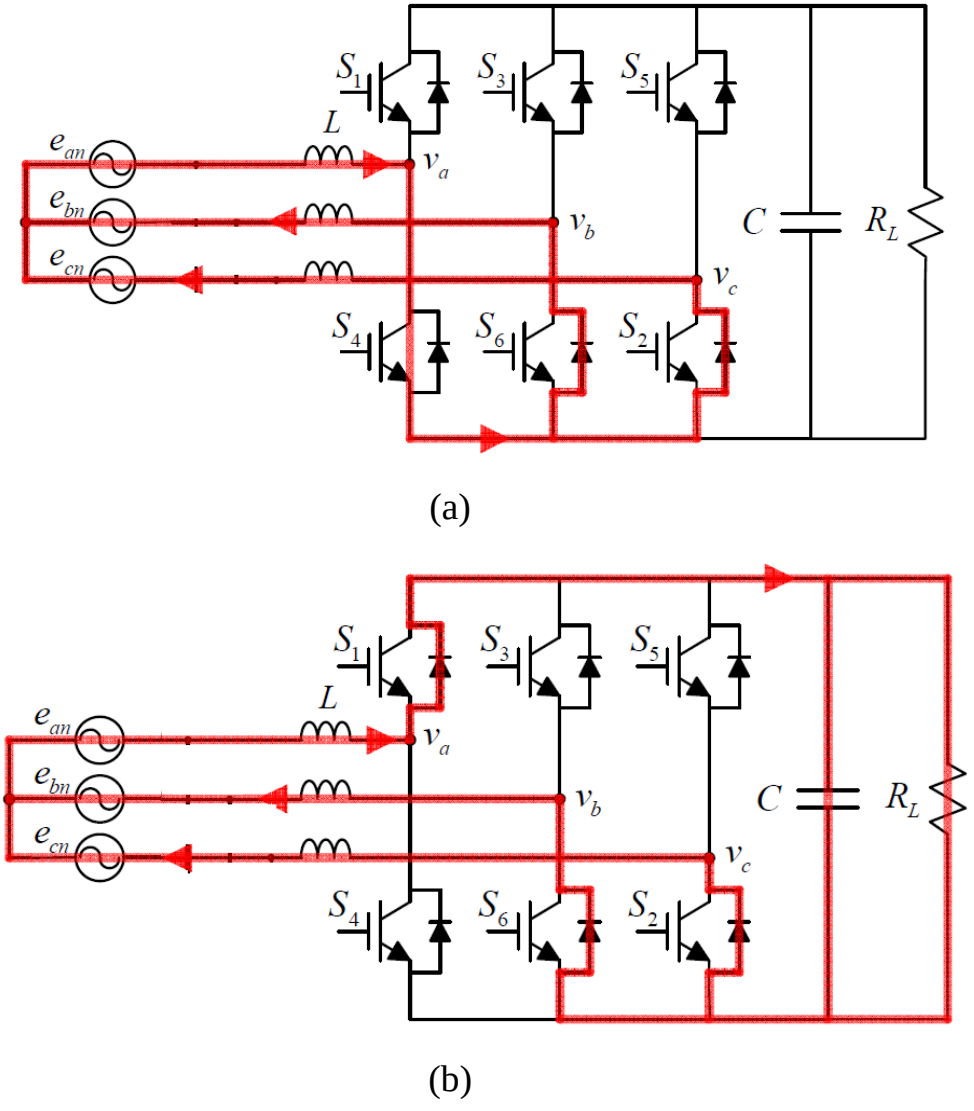

Figure 2.2: The directions of the current through switching state [12].

The simplified per-phase equivalent circuit of the rectifier has been represented in Fig. 2.3 Here, V_i signifies the single phase grid voltage and V_{ri} represents the per-phase rectifier input voltage.

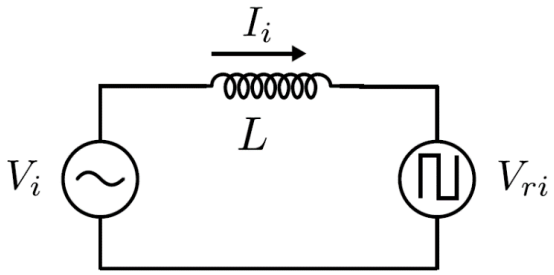

Figure 2.3: Single phase equivalent circuit of the rectifier

The analysis of simplified per-phase equivalent circuit is constrained to quantities at fundamental frequency alone, the per-phase rectifier input voltage can be written as,

$$V_{ri} = V_i - j\omega_o L I_i \quad (1)$$

Where,

$$V_i = V_m cos(\omega t) \quad (2)$$

The current through the inductor is done by the voltage difference across it and for the case of UPF operation, the current can be written as,

$$I_i = I_m cos(\omega t) \quad (3)$$

The control of this current is done by controlling the voltage difference across the inductor which is given by the difference of the grid voltage V_i and the rectifier input voltage V_{ri}. The voltage V_{ri} is controlled at the required phase and magnitude by appropriate switching of the bi-directional switches S_i using hysteresis controller. The current ripple at these high switching frequencies is attenuated to a great extent by the line and filter inductances.

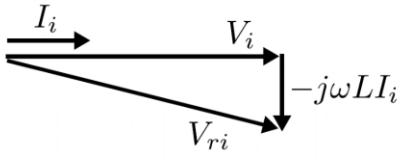

Figure 2.4: Phasor diagram for UPF operation

From the phasor diagram in Fig.2.4, it can be seen that the magnitude of the rectifier input voltage V_{ri} is greater than the input grid voltage, illustrating the `boost' nature of the rectifier. Thus the DC output voltage that can be obtained from the rectifier can only be greater than the peak value of the input line-line voltage.

The DC power delivered to load under UPF operation is given by power balance as (neglecting the system losses),

$$P_{dc} = V_{dc}I_{dc} = (3/2)V_mI_m \qquad (4)$$

2.2 Hysteresis band Current Control Scheme

As discussed earlier, the control structure of a three-phase six-switch boost converter consists of an inner current control loop and an outer voltage control loop. The dc link capacitor voltage V_{dc} is sensed and compared with the desired value V_{dc}*. This error is processed by a proportional–integral (PI) controller to generate a signal I_{peak}*. This I_{peak}* is magnitude of reference current for input AC side. To generate reference current for a phase, the magnitude of reference current of a phase is multiplied with unit sine vector template, which can be obtained by dividing the phase voltage of that phase with it's peak value. The current controller senses the input current and compares it with a sinusoidal current reference. The error signal is then sent to the hysteresis relay and accordingly switching takes place. Fig.2.5 shown below describes the control strategy for switches S_1 and S_4 which are connected to phase 'a'.

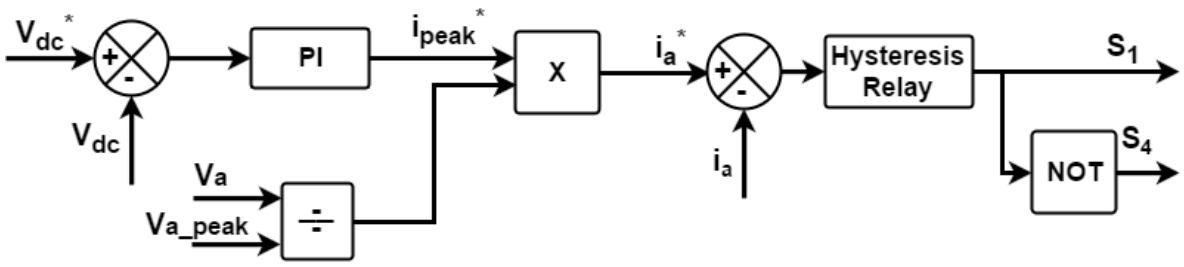

Figure 2.5: Hysteresis Band Control scheme for boost rectifier topology

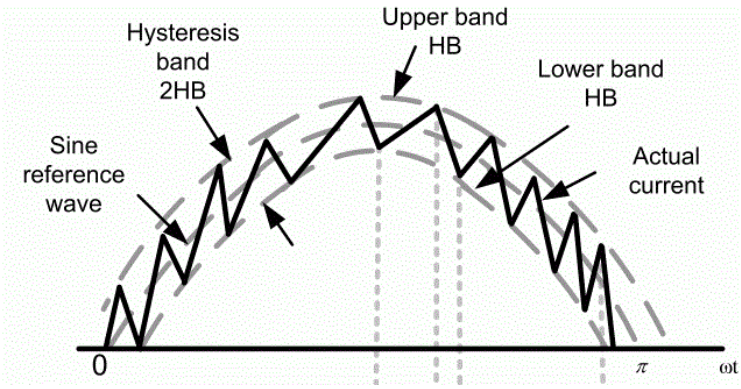

Figure 2.6 - Hysteresis band current control

The advantages with hysteresis band current control scheme are it's excellent dynamic response, low cost and easy implementation. But variations in switching frequency are observed in this scheme which raises concerns over it's practicality while working with the IGBT and MOSFET switches.

For limiting the switching frequency the hysteresis band relay can be replaced by triangular carrier Pulse width modulation as in the Fig. 2.5 below. This scheme also assists in designing the boost inductor more accurately.

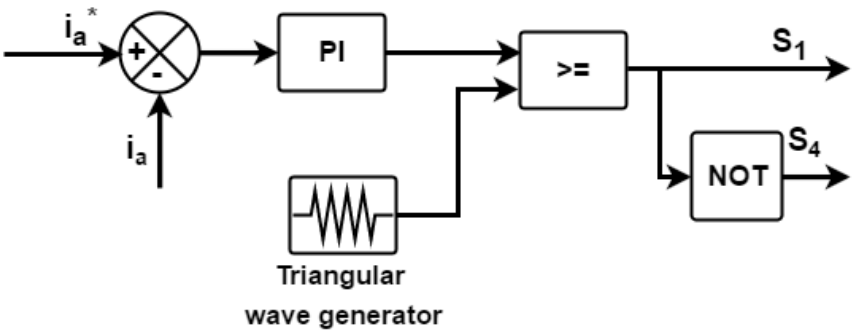

Figure 2.7: PWM Control scheme for boost rectifier topology

2.3 Boost Inductor Design

The value of Boost inductor L is decided by limiting the voltage drop across it and also from the switching frequency current ripple. Since we don't have a fixed switching frequency in Hysteresis control, the first option is considered here. Voltage drop across the inductor is limited to 5% of the per phase input voltage (110V).Assuming a purely sinusoidal input current it can be seen that the voltage drop across the inductor is given by,

$$\omega L I_a = 5.5V \qquad (5)$$

$$L = 22mH$$

Which means that an inductance of value less than 22 mH has to be chosen to limit the voltage drop across the inductor to 5% of the input voltage.

2.4 DC Link Capacitor Design

The DC link capacitor absorbs current-ripple and provides a stable voltage at the output end. During conduction mode of operation capacitors charges by a current at this moment $I_L = I_C$. Considering a permissible voltage-ripple (ΔV_C) to around 3% - 5% at peak-power during the time period T_0, the capacitor value can be estimated using expression (5).

$$C = I_L * (T_0 / \Delta V_C) \text{ , Where, } \Delta V_C \text{ is 5\% of } V_{dc} \qquad (5)$$

CHAPTER 3: DC MICROGRID CONFIGURATION

A DC microgrid can be perceived as a distribution network incorporating a wide range of distributed generation systems, largely non-conventional renewable energy sources and DC storage systems with local loads. DC microgrid is an effective method to reduce the losses in the system with high reliability. It can eliminate multiple power conversion stage and therefore it has advantages in the stand of efficiency, cost and system size. The absence of reactive power and possibility of an efficient integration of small distributed generation units inspires the idea of DC microgrid. Also the fact that, internally, most of the loads operate using a DC voltage. DC microgrid is suitable for domestic needs which are mainly of DC loads.

As shown in Fig. 3.1, the proposed DC microgrid for the project comprises photovoltaic generation system as non-conventional renewable energy source, battery energy storage element, DC loads and grid tied converter.

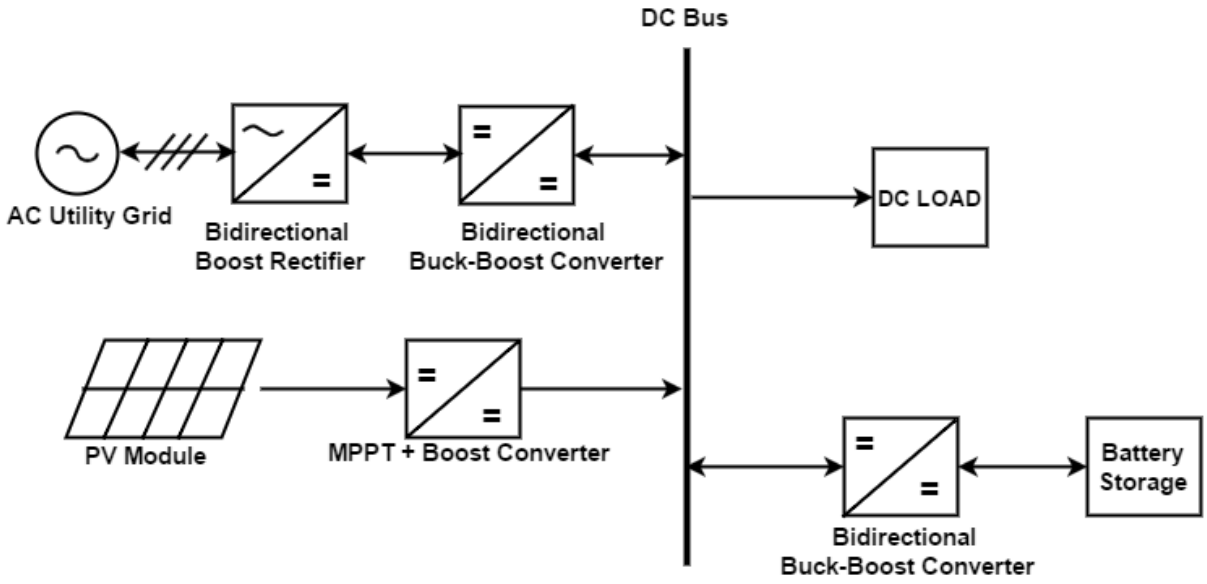

Figure 3.1: DC microgrid configuration

3.1 Photovoltaic Module

Photovoltaic panels are composed of PV cells which are made of semiconducting materials that exhibit the photovoltaic effect. In PV cells, sunlight is absorbed and results in excitation of electron or charge carrier to higher energy state from valence band to conduction band and thus allowing the flow of current and production of electrical potential. At present single crystalline silicon and amorphous or thin film silicon are the most popularly used materials in photovoltaic panels. Due to technological advances in manufacturing and scaling in production, the cost of producing PV cells has been dropped. The series and parallel configurations of PV panels are used to fulfil energy requirement. When several PV cells are connected in series and parallel connections then it is called PV array. Series connected cells are used to increase the voltage rating of PV panel whereas the parallel connected cells are accountable to increase the current rating of the PV panel.

3.1.1 Modelling of PV module

Modelling of PV module is based on a single diode equivalent model considering the irradiation and temperature as per the nominal condition. Fig. 3.2 shows the equivalent circuit of a PV panel with connected R load.

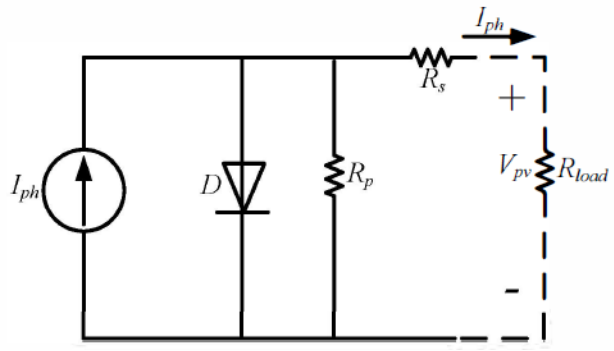

Figure 3.2: Equivalent circuit of a PV panel

Equations (6)-(8) show the mathematical model of the PV panel and its output current.

$$I_{pv} = n_p I_{ph} - n_p I_{sat} \cdot [\exp((\frac{q}{AkT})(\frac{V_{pv}}{n_s} + I_{pv} R_s)) - 1] \quad (6)$$

$$I_{ph} = (I_{sso} + ki(T - T_r)) \cdot \frac{S}{1000} \quad (7)$$

$$I_{sat} = I_{rr} (\frac{T}{Tr})^3 \exp((\frac{qE_{gap}}{kA}) \cdot (\frac{1}{T_r} - \frac{1}{T})) \quad (8)$$

The PV system naturally exhibits a nonlinear I-V and P-V characteristics which vary with the radiant intensity and cell temperature [13]. These characteristics of PV system are illustrated in the Fig. 3.3 shown below. The open circuit voltage V_{OC} will be produced when there is no load connected to PV panel and undoubtedly with zero current. The short-circuit current I_{SC} can be measured when the output terminal of PV panel are shorted together resulting in zero output voltage. In both scenarios, no power is delivered by the PV panel. In the I-V curve the maximum power point can be spotted near the knee point. The voltage and current at the maximum power point are designated as V_m and I_m.

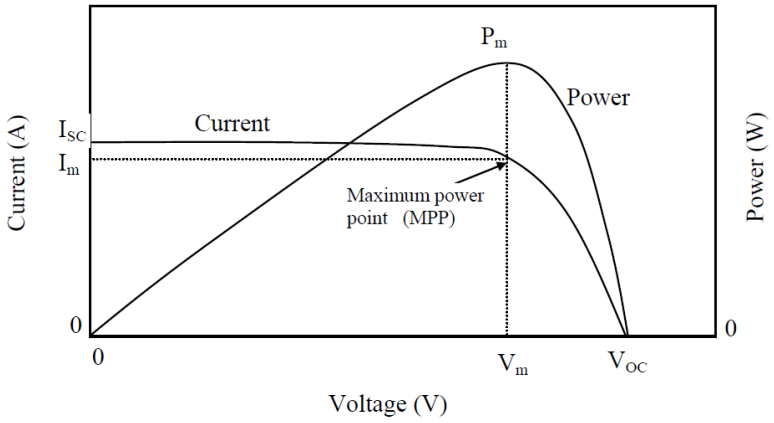

Figure 3.3: I-V and P-V Characteristics of Solar Panel

3.1.2 MPPT Control by Perturb and Observe method on Boost Converter

As discussed earlier, the output power of PV system vary with the radiant intensity and cell temperature. To obtain the maximum power point at a given point of time MPPT(Maximum power point tracking) algorithms are implemented with a DC-DC converter with PV module as

the input source. One of the most widely used MPPT algorithm is Perturb and Observe technique. In this technique, the PV voltage and current are measured and the output power is calculated. A small perturbation of voltage ΔV or duty cycle ΔD is incorporated in the system through DC-DC converter in one direction (positive or negative ΔV). If new output power calculated is greater than previous power then perturbation is in correct direction otherwise it should be reversed. Fig. 3.4 describes the flow chart of P&O MPPT algorithm.

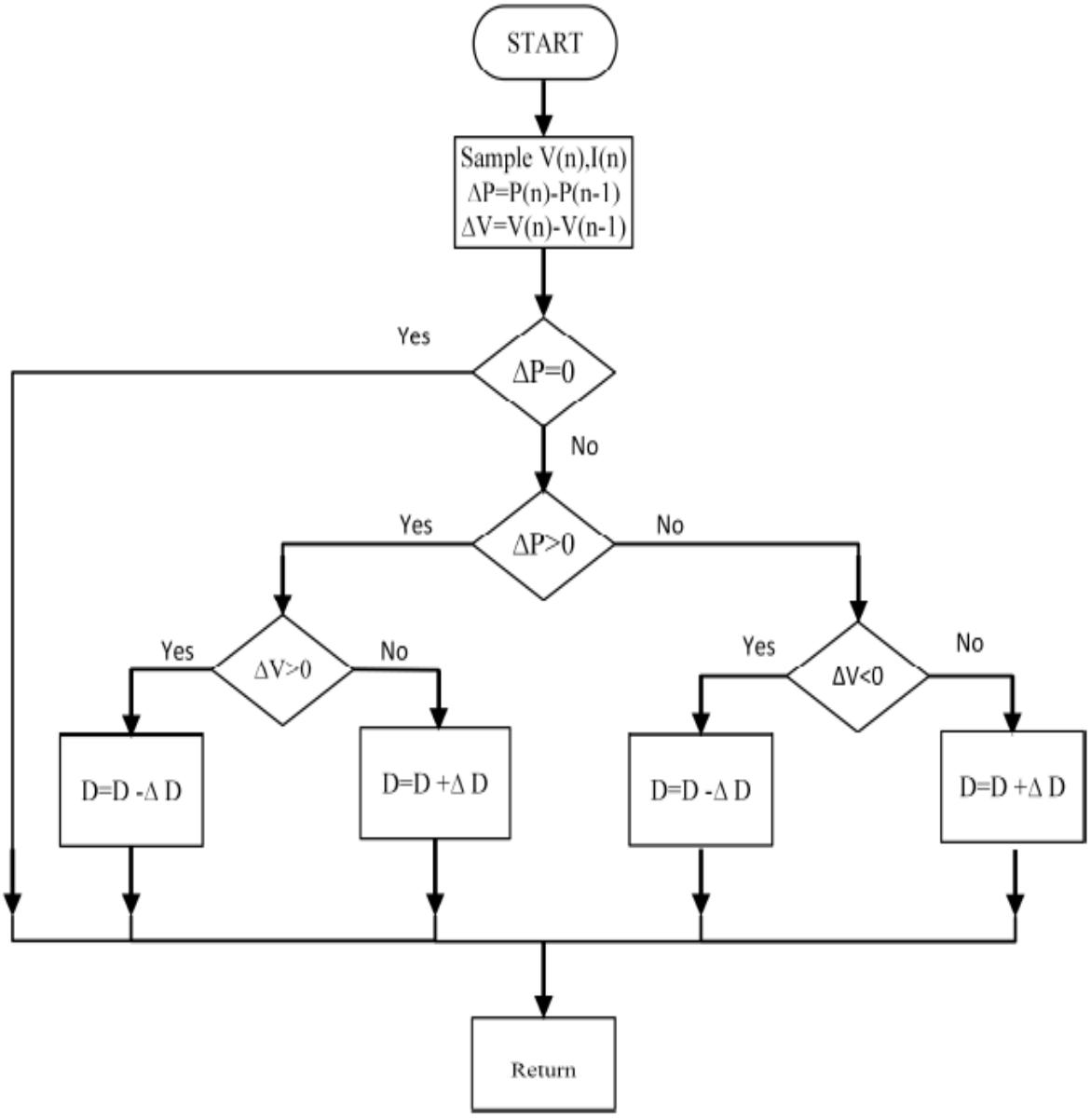

Figure 3.4 – Flow chart for P&O method of MPP

MATLAB code for P&O MPPT algorithm

```
function D  = PandO(V, I)

% MPPT controller based on the Perturb & Observe algorithm.

% D output = Duty cycle of the boost converter (value between 0 and 1)
% V input = PV array terminal voltage (V)
% I input = PV array current (A)
%
% Param input:
Dinit = 0.4;  %Initial value for D output
Dmax = 0.9;   %Maximum value for D
Dmin = 0.1;   %Minimum value for D
deltaD = 0.0001; %Increment value used to increase/decrease the duty cycle D
% ( increasing D = decreasing Vref )

persistent Vold Pold Dold n ;

dataType = 'double';

if isempty(Vold)
    Vold=0;
    Pold=0;
    Dold=Dinit;
end

P= V*I;
dV= V - Vold;
dP= P - Pold;

if (dP>2) || (dP<-2 )
    if dP < 0
        if dV > 0
            D = Dold - deltaD;
        else
            D = Dold + deltaD;
        end
    else
        if dV < 0
            D = Dold + deltaD;
        else
            D = Dold - deltaD;
        end
    end
else D=Dold;
end

if D >= Dmax || D<= Dmin
    D=Dold;

end

Dold=D;
Vold=V;
Pold=P;

end
```

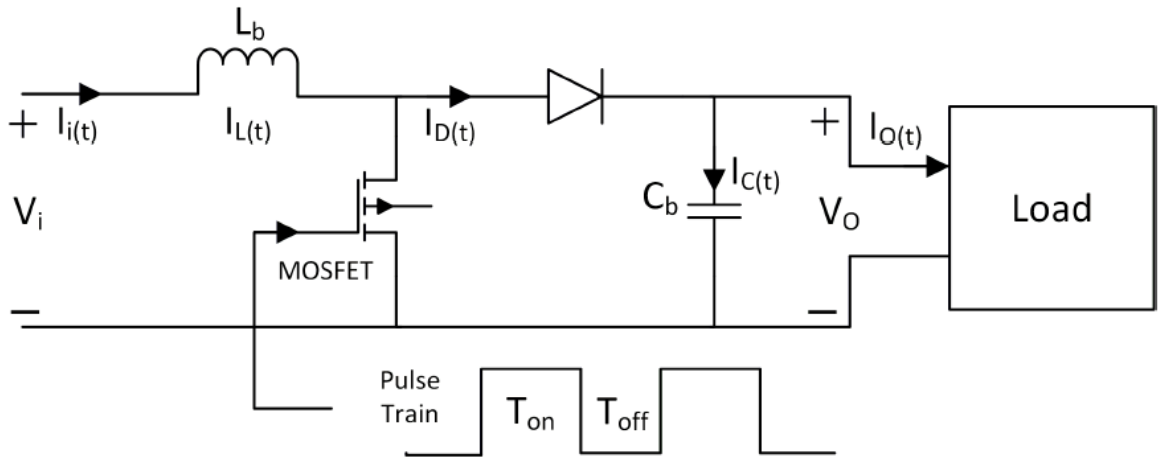

Figure 3.5: Circuit Schematic of Step-up DC/DC Converter

The topology presented in this application of P&O maximum power point tracking is a boost converter[13]. The schematic diagram of boost converter is shown in Fig. 3.5. The boost converter is a special case, in consideration of it's non-linear dynamic behaviour transfer function during Continuous Conduction Mode (CCM) operation.

In the MPPT mode operation PV system generates maximum output power which can be supplied to load and excess power can be used for energy storage or can be fed to utility grid through bidirectional converter. In constrained mode operation the PV system generates less than maximum power.

3.2 Battery Energy Storage System

In the structure of DC microgrid presented in the project the energy storage elements can switch between charge, discharge and off mode in order to maintain DC microgrid power balanced. In order to protect and ensure the life time of the storage elements, the operation of storage elements must range between set maximum and minimum value of SOC (SOC_{min} & SOC_{max}). A flow diagram was developed and implemented in Stateflow of MATLAB Simlink for control of charging and discharging of the battery. The battery is chosen such that the nominal voltage of the battery is less than the DC microgrid bus voltage.

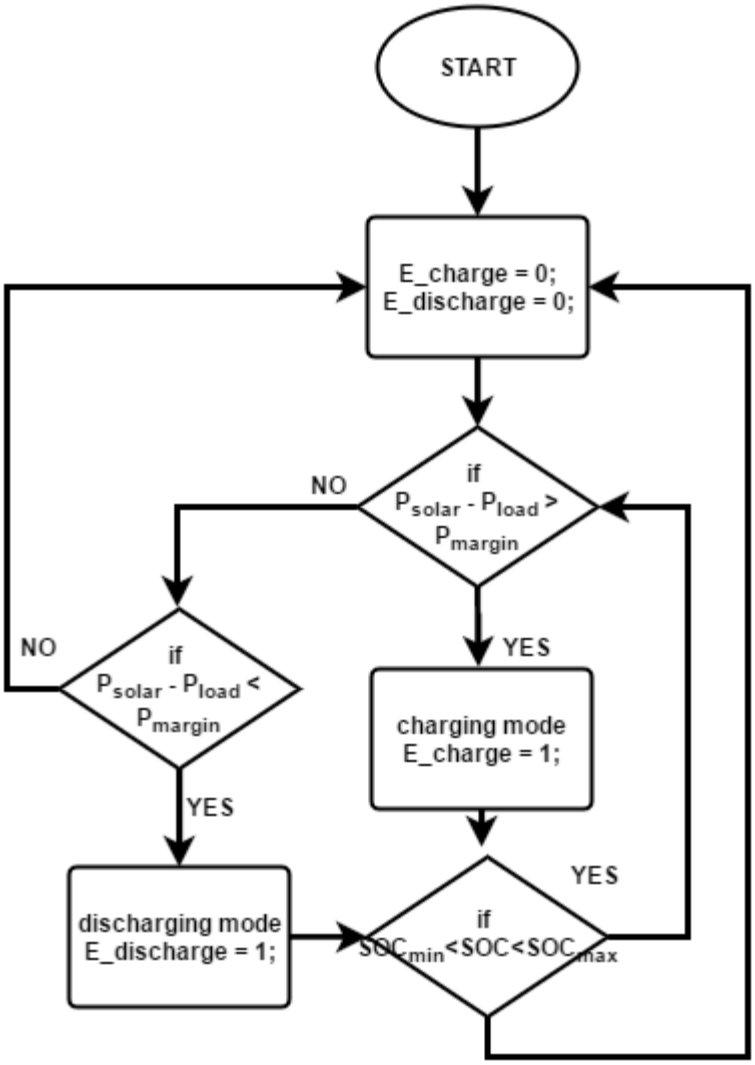

Figure 3.6: Flow chart for charging and discharging of battery.

The stateflow control gives two output signals named E_charge, which enables the charging of the battery, and and E_discharge, which enables the discharge of the battery. Both the signals are used in the bidirectional buck boost converter which manages the charging and discharging of the battery. The circuit of bidirectional converter is shown in Fig 3.7 .

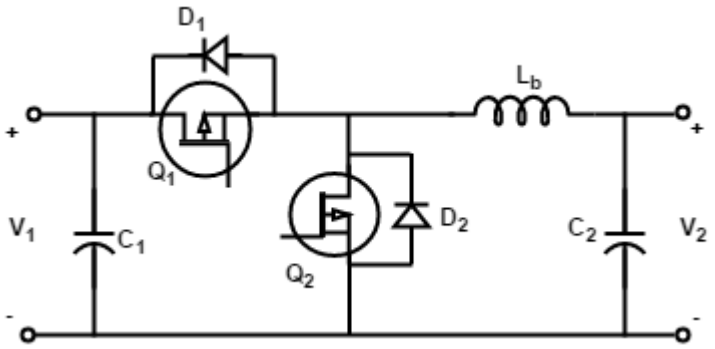

Figure 3.7: Circuit Schematic of Bi-directional DC-DC Converter

During the charging time the converter works as a buck converter and the power flow is controlled by the current controller which manages a constant current charging. In buck operation the buck switch Q_1 and diode D_2 manages the power flow.

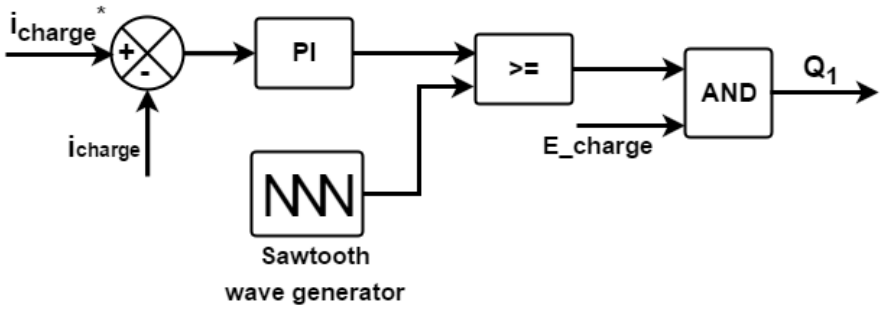

Figure 3.8: Control Scheme for switching of Converter during charging of the battery

During the discharging time the converter operates as boost converter and power flow is controlled by voltage control loop which manages the DC bus voltage to it's reference value.

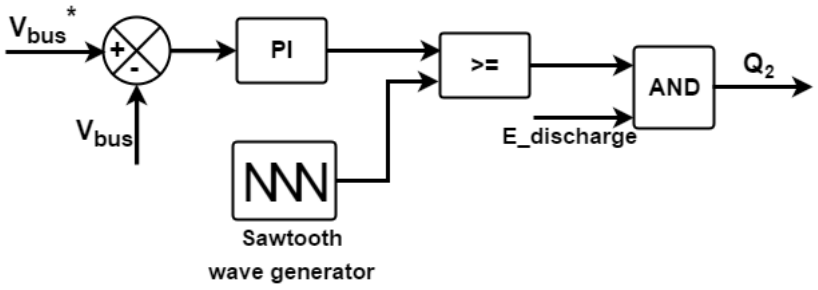

Figure 3.9: Control Scheme for switching of Converter during discharging of the battery

3.3 AC-DC bidirectional PFC circuit

A three phase six switch boost rectifier is associated with a bidirectional buck-boost DC-DC in cascade connection in the presented DC microgrid configuration. The basic functioning of AC-DC converter has been already described in the chapter 2. During the rectifier operation the bidirectional DC-DC converter operates as buck converter and in inversion mode the DC-DC converter operates as boost converter. The voltage is stepped-up first by boost rectifier above the DC bus voltage and then stepped down to the DC bus voltage. The first stage i. e. boost rectifier supervises the power quality of utility grid and the second stage manages the power flow between utility grid and DC microgrid.

The control scheme for bidirectional DC-DC buck boost converter is shown below in Fig. 3.10 . This scheme controls the output current to DC microgrid. The power demand of load is compared with the generated solar power and the required power or excess power is calculated. This mismatch between the generated power and load power is handled by bidirectional converter[14].

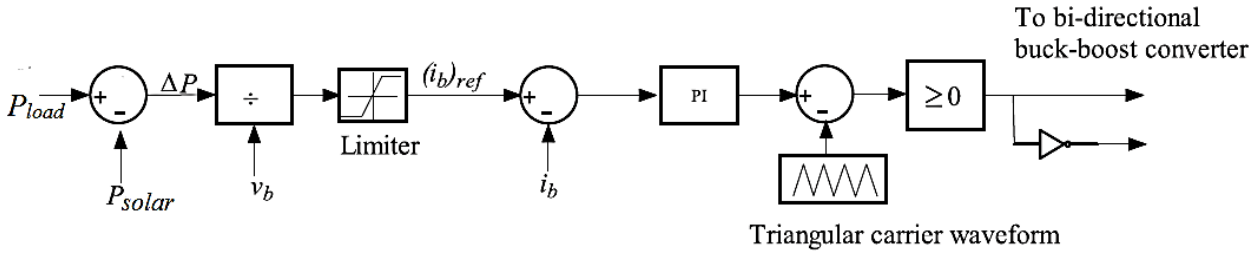

Figure 3.10: Control Scheme for Boost rectifier connected bidirectional DC-DC Converter

3.4 Power flow management

The generating sources consisting of photovoltaic array, energy storage and ac grid are depicted in Fig. 3.1. The power supply from photovoltaic source to the DC-microgrid is unidirectional. The battery energy storage smoothens the power balances of the DC-microgrid by charging and discharging. Hence the power flow between the battery and the microgrid is bidirectional but it can't exchange power with AC grid. The power from battery is supplied to load in case of deficient power generation from PV module or provided from PV module in case of excess power generation from PV module. The excess power from PV module can be sent to AC utility grid or in case of power deficiency power can be extracted from the AC utility grid.

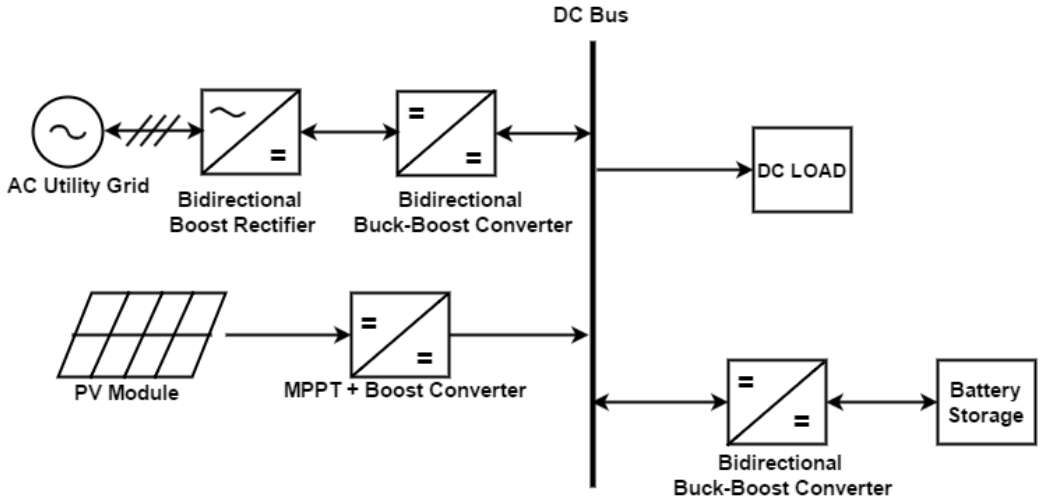

Figure 3.11: Power Flow in DC microgrid configuration

CHAPTER 4: PERFORMANCE INVESTIGATION USING MATLAB SIMULATION

A three phase bidirectional boost rectifier with bidirectional buck-boost converter is studied for DC microgrid application. First the six switch boost rectifier with PWM current control was implemented for a DC load. Then the six switch bidirectional boost rectifier was implemented with bidirectional buck-boost converter and Photovoltaic generation. The operation of PFC circuit was studied for both rectifier and inverter mode by changing the load conditions and power generated from PV module. Also the flow diagram of charging and discharging of battery energy storage system in islanded mode was implemented with Stateflow in MATLAB/Simulink environment.

4.1 Simulation of three phase six switch boost rectifier for DC load

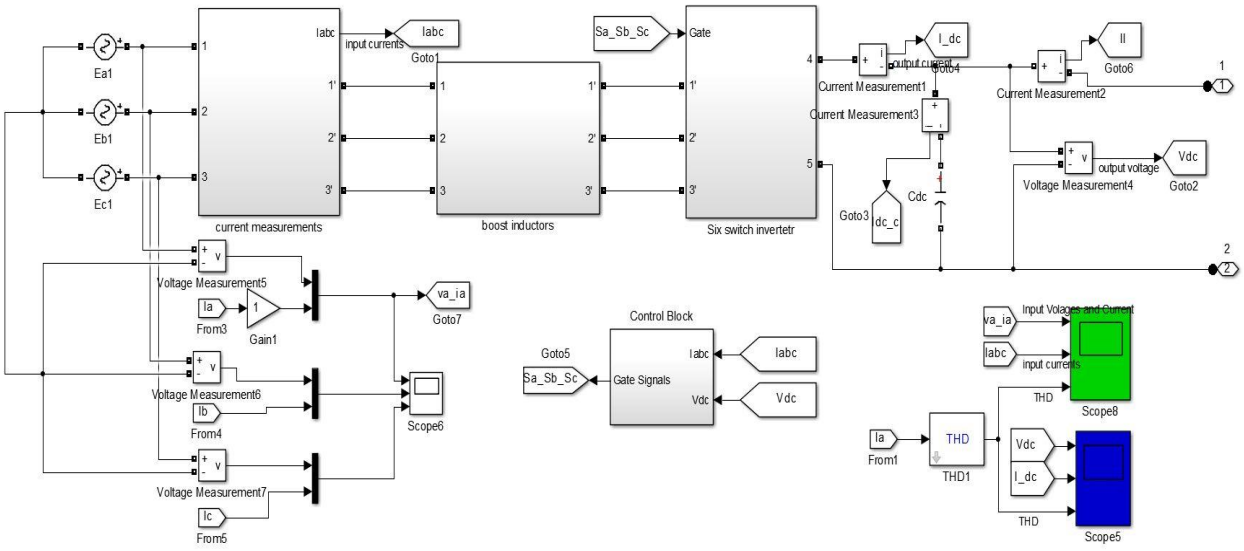

Figure 4.1: Complete Simulink model of three phase six switch boost rectifier

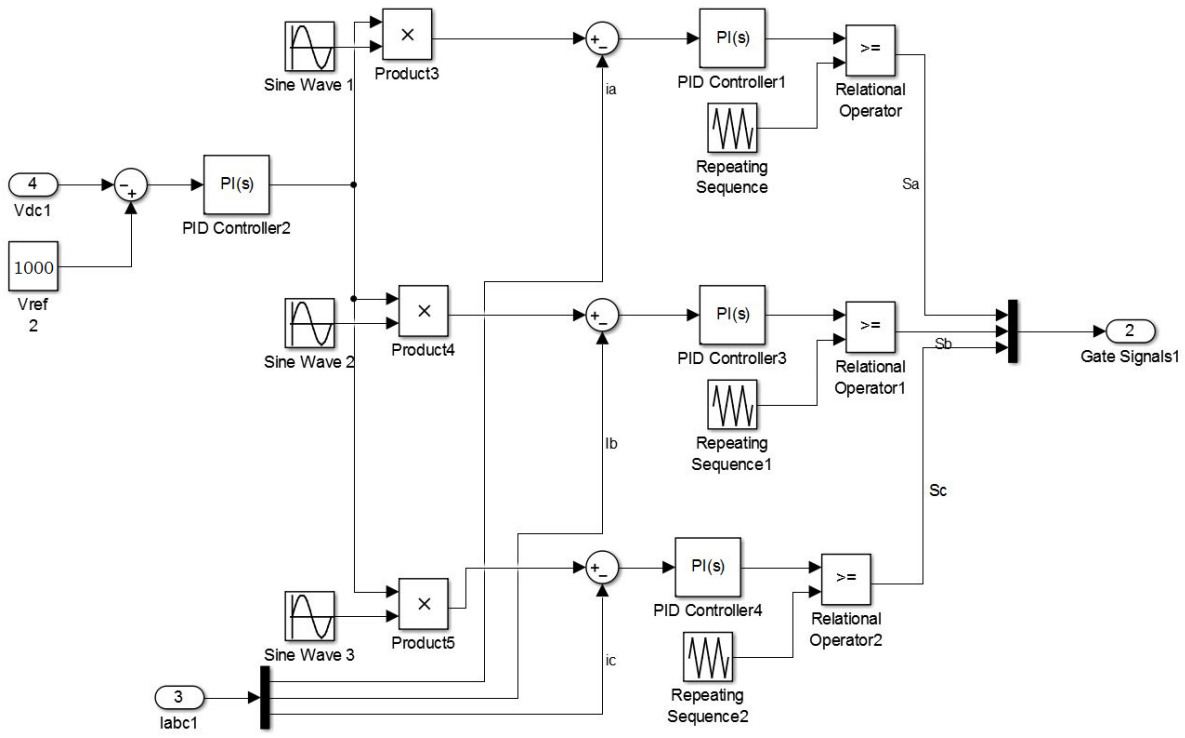

Figure 4.2: PWM Control block of three phase six switch boost rectifier

Table 4.1: Simulation parameter chosen for three phase six switch boost rectifier

Description	Rating
Line-Line Input Voltage V_{ll}	415 V
DC output VoltageV_{out}	1000 V
Boost Inductor L	4 mH
Damping resistor R	0.01 ohm
DC link Capacitor C	2000uF
PWM triangular wave frequency f_S	5kHz
DC load	25 kW

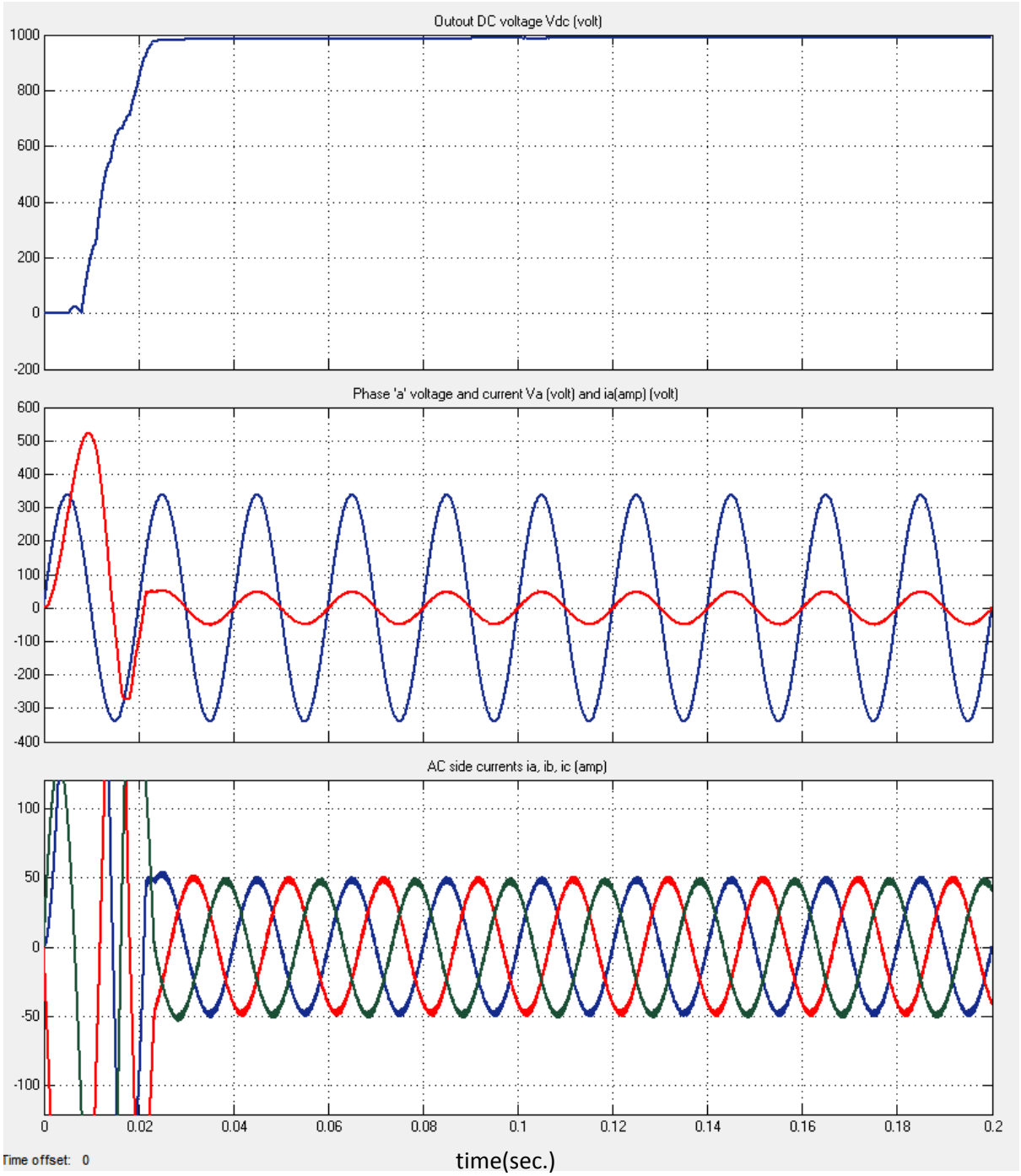

Figure 4.3: Simulation results of three phase six switch boost rectifier for dc load.

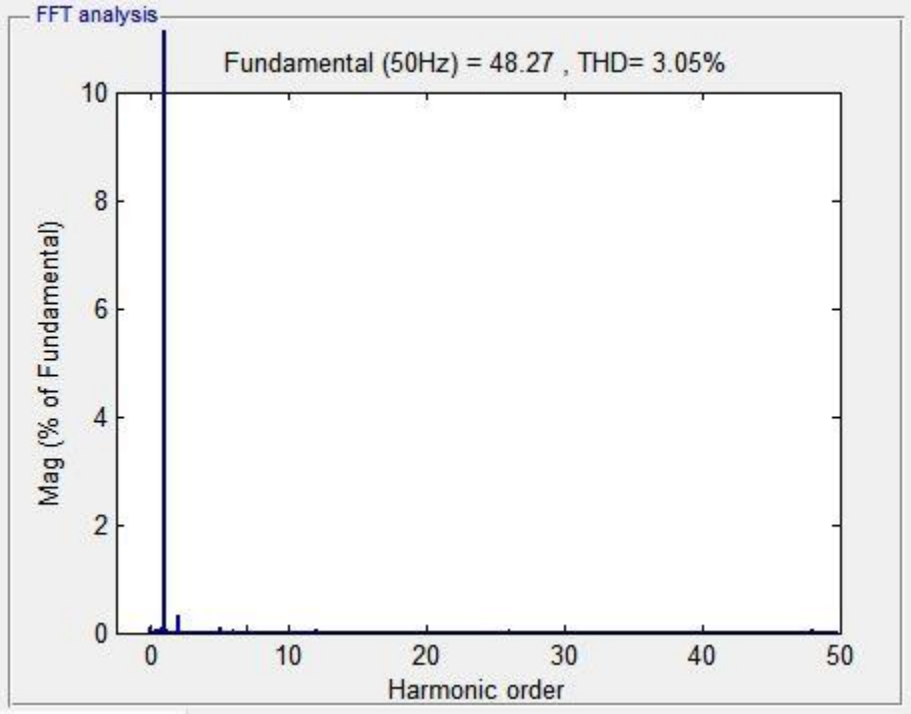

Figure 4.4: FFT analysis of ac side current i_a for simulation of three phase six switch boost rectifier for dc load.

In this simulation the AC-DC six switch boost active rectifier was used to feed a DC load of 25kW. The boost voltage was controlled to 1000V. Unity power factor operation was manages by the PWM current controller. The THD of phase 'a' current i_a was restricted to 3.05%.

4.2 Simulation Results for load change with constant power generation from PV module in DC microgrid

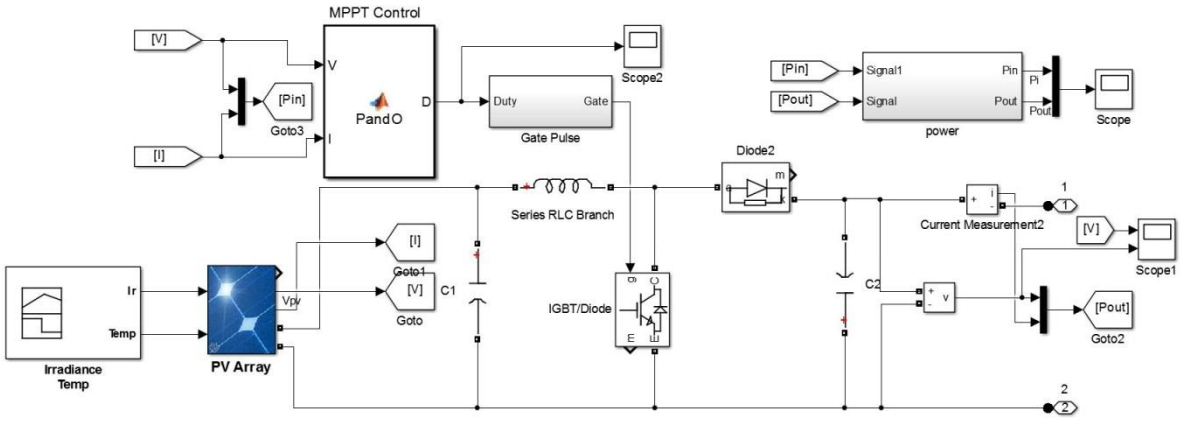

Figure 4.5: Simulink model of PV module with MPPT

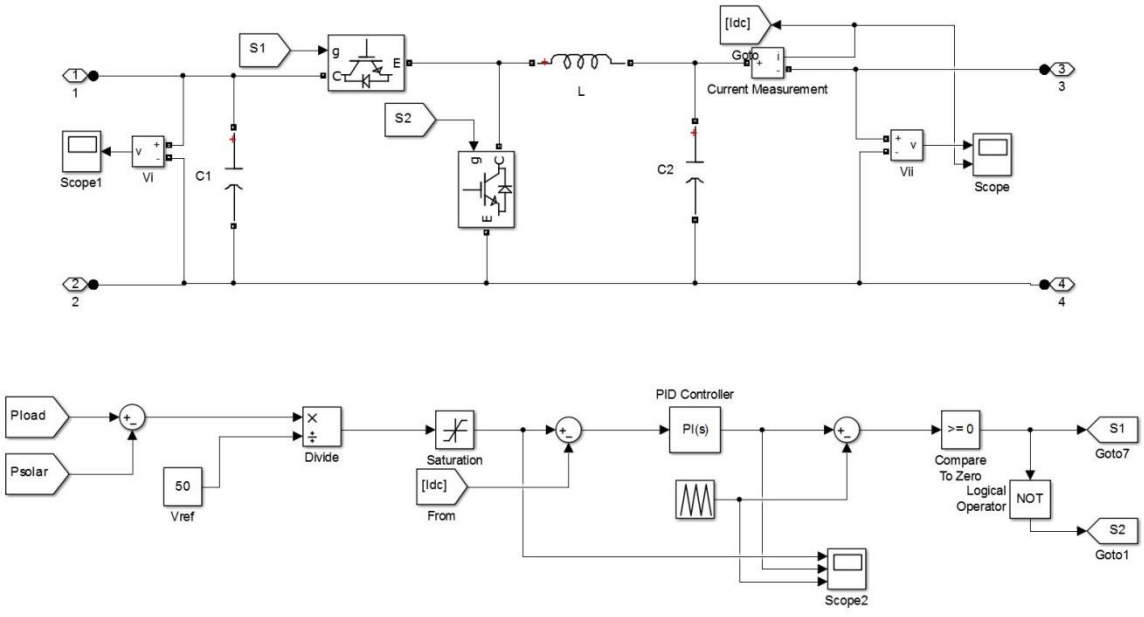

Figure 4.6: Simulink model of Bidirectional DC-DC converter

Table 4.2: Simulation parameters chosen for DC microgrid application

Description	Rating
DC bus voltage V_{dc_bus}	50 V
Line-Line Input Voltage V_{ll}	110 V
Boost Rectifier Output VoltageV_{boost}	400 V
Boost Rectifier Inductor L_b	10 mH
Damping resistor R in Boost rectifier	0.01 ohm
DC link Capacitor C in Boost rectifier	1000uF
Switching frequency of Bidirectional converter f_{S_bb}	10kHz
DC load connected at DC microgrid bus	800 W, 1600 W
PV module	SunPower SPR-305 WHT
Number of series-connected modules per string	1
Number of parallel strings	5

This simulation is focused on the operational characteristics of DC microgrid in the condition of load change which involves power flow from three phase utility grid. Initially, a DC load of 800 W is connected to the DC microgrid of 50 V bus voltage. During this period of time the load requirement is lower than the power generated from PV module. The PV module is operating in MPPT mode. The excess power is fed to the three phase utility grid through inversion operation of PFC circuit . After t = 2sec, load is increased to 1600 W. In this scenario the load demand is more, so the remaining power is supplied by utility grid through rectification operation of PFC circuit.

From t = 0 sec. to t = 2 sec.

Power requirement of load, P_{Load} = 800W;

Power generated by PV System, P_{Solar} = 936 W at Irradiance 800 W/m2

Power sent back to Grid, P_{grid} = 136 W;

After t = 2 sec.

Power requirement of load, P_{Load} = 1600W;

Power generated by PV System, P_{Solar} = 936 W at Irradiance 800 W/m2

Power supplied by Grid, P_{grid} = 664 W;

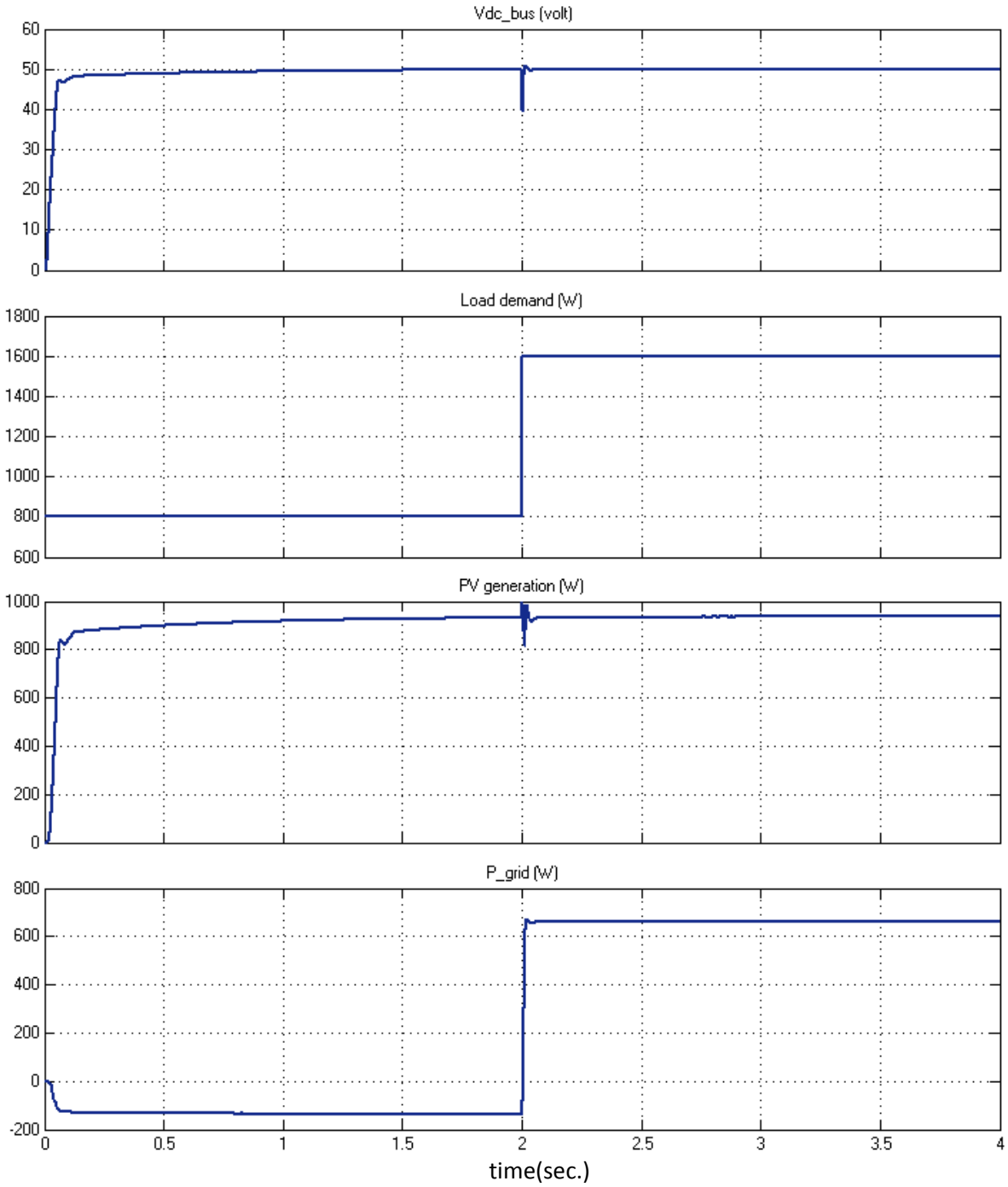

Figure 4.7: Simulation results of power flow of DC microgrid operation for load change with constant power generation from PV module.

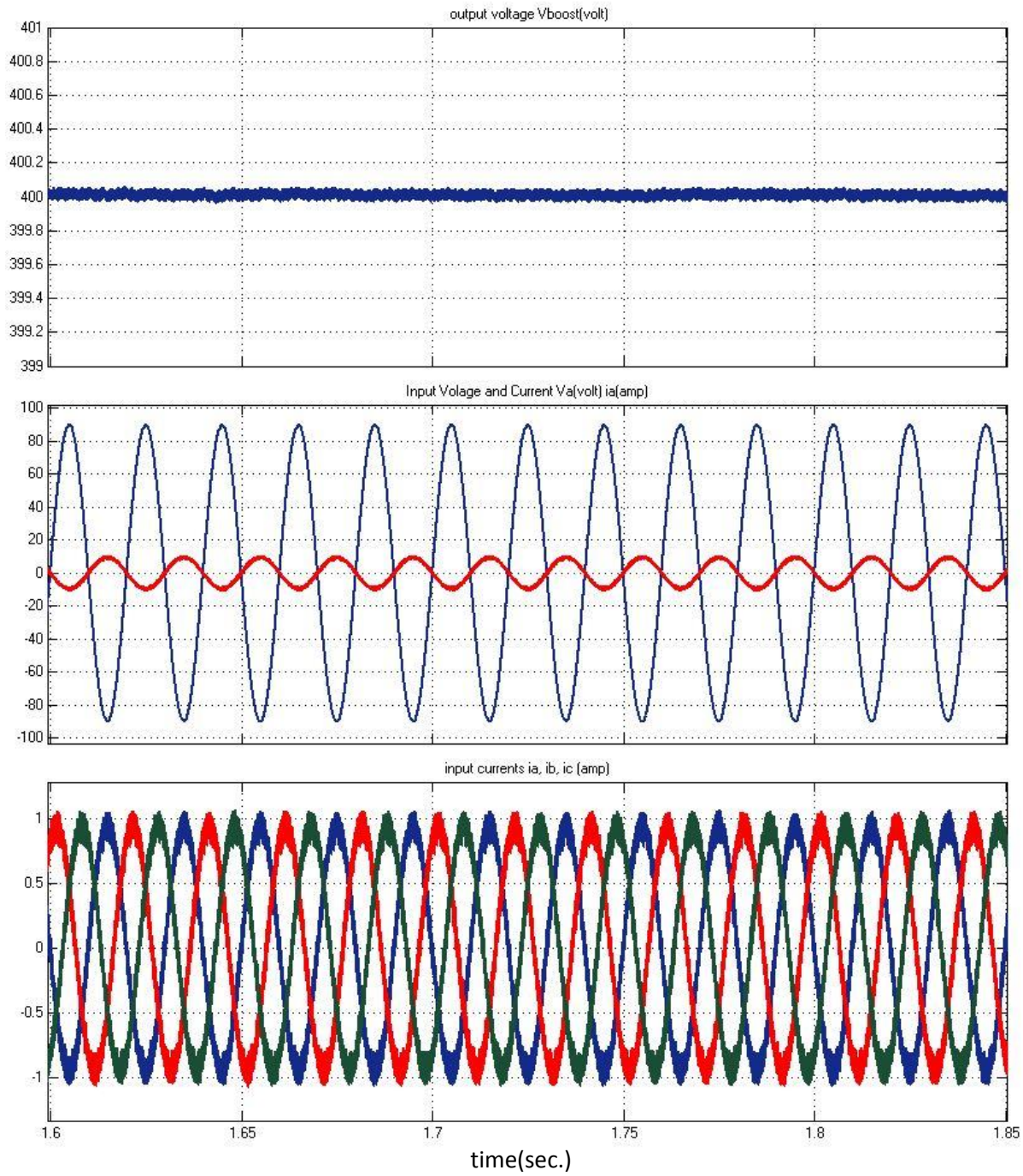

Figure 4.8: Simulation results of output boost voltage and ac side waveforms in inversion mode operation of PFC circuit

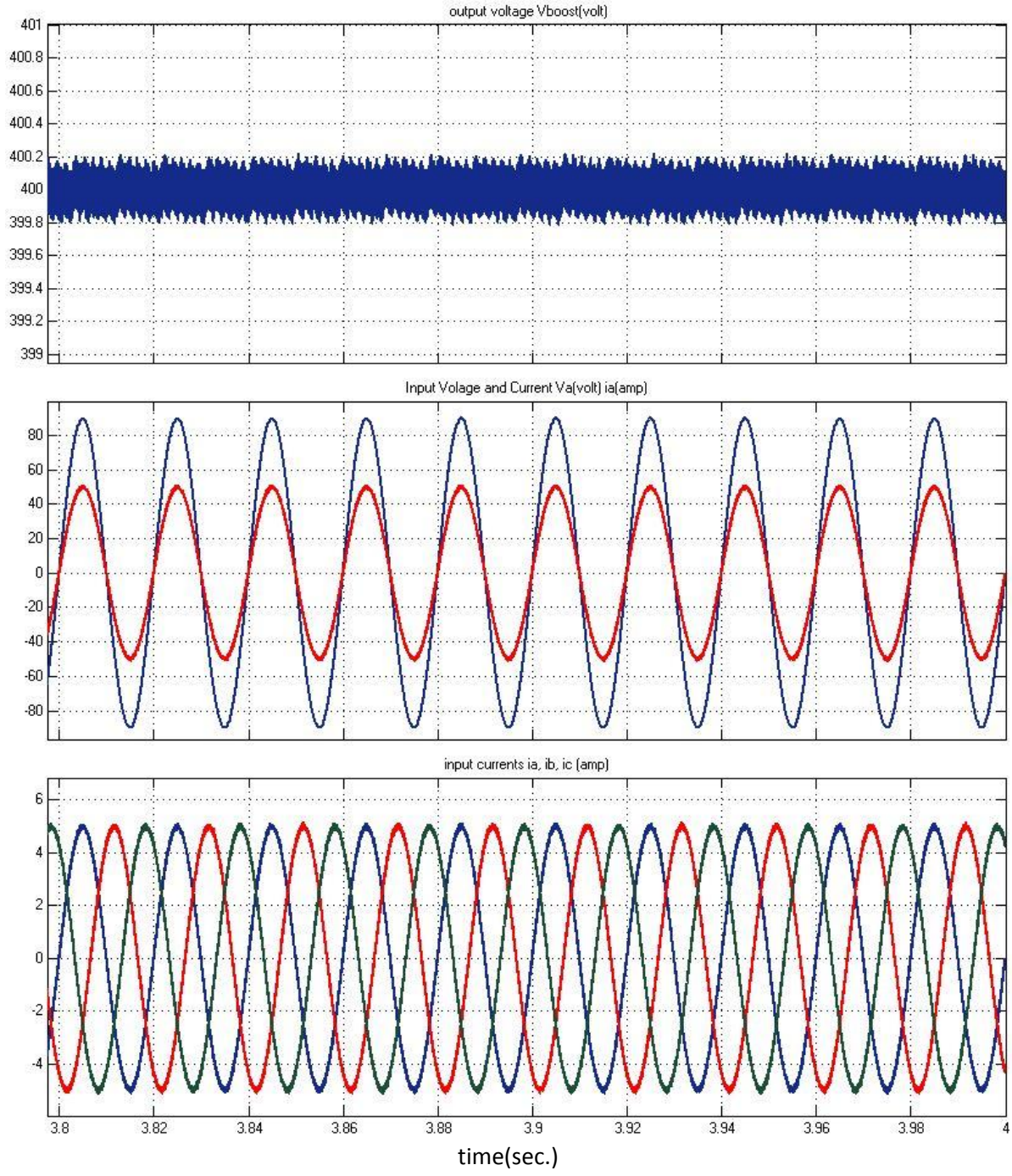

Figure 4.9: Simulation results of output boost voltage and ac side waveforms in rectification mode operation of PFC circuit

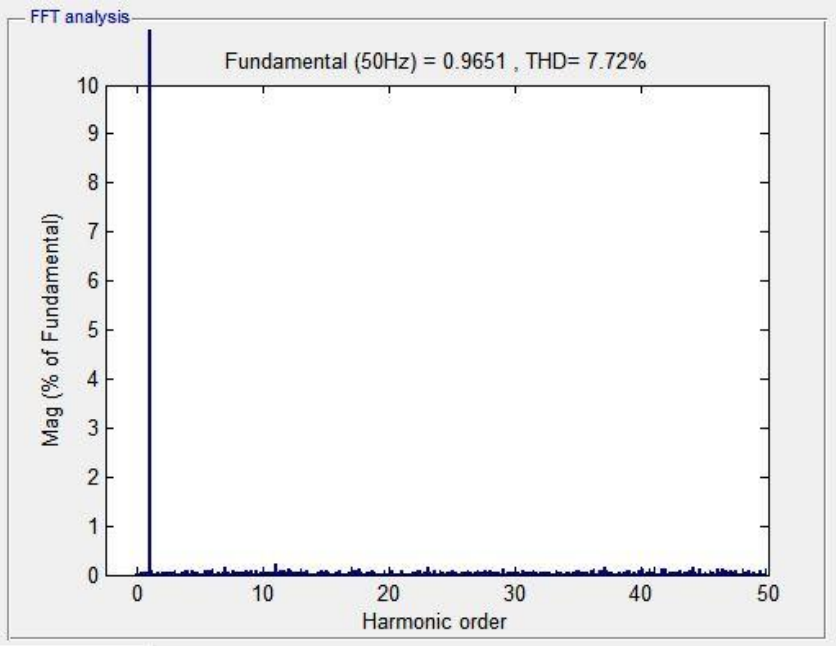

Figure 4.10: FFT analysis of ac side current i_a during inversion mode operation of PFC circuit.

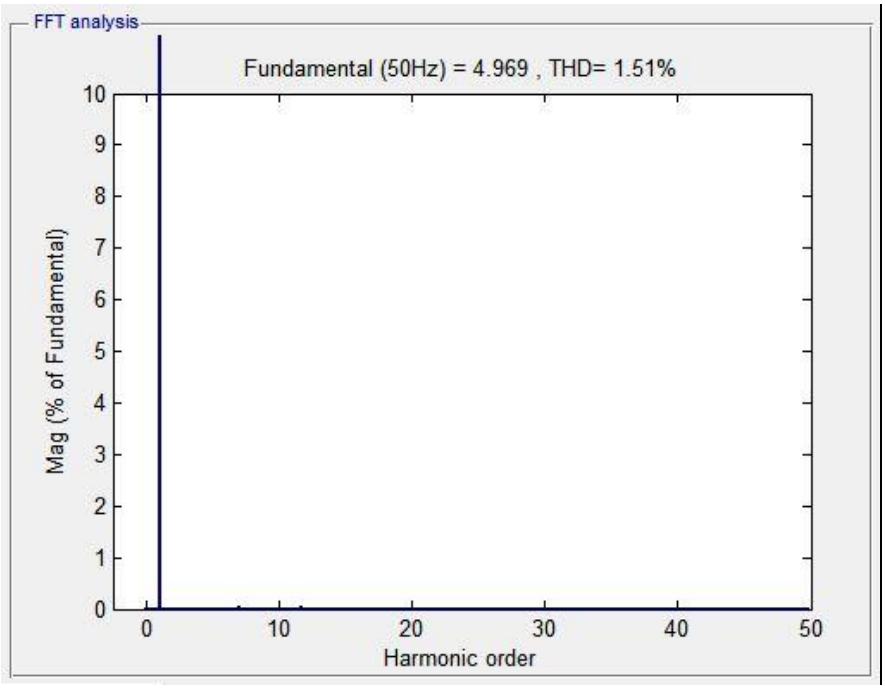

Figure 4.11: FFT analysis of ac side current i_a during rectification mode operation of PFC circuit.

4.3 Simulation Results for constant load and variable power generation from PV module in DC microgrid

This simulation is focused on the operational characteristics of DC microgrid in the condition of variation in generated power from PV module, which involves power flow from three phase utility grid. A DC load of 250 W is connected to the DC microgrid of 50 V bus voltage. During this period of time the load requirement is lower than the power generated from PV module. The PV module is operating in MPPT mode. The excess power is fed to the three phase utility grid through inversion operation of PFC circuit. After t = 2sec, the intensity of light changes and results in decrement of power generation of PV module. The PFC circuit reacts accordingly to match the power requirement. The simulation parameters are same as described in Table 2, except the required load which is 250W throughout in this case and irradiance to PV panel is 750 W/m^2 for t = 0 sec. to t = 2 sec and constantly decreasing after that.

From t = 0 sec. to t = 2 sec.

Power requirement of load, P_{Load} = 250W;

Power generated by PV System P_{Solar} = 830 W at Irradiance 750 W/m2

Power sent back to Grid P_{grid} = 580 W;

After t = 2 sec.

Power requirement of load, P_{Load} = 250W;

Power generated by PV System P_{Solar} = decreasing due to decrement in irradiance

Power fed by Grid P_{grid} = continuously increasing to match the load requirement

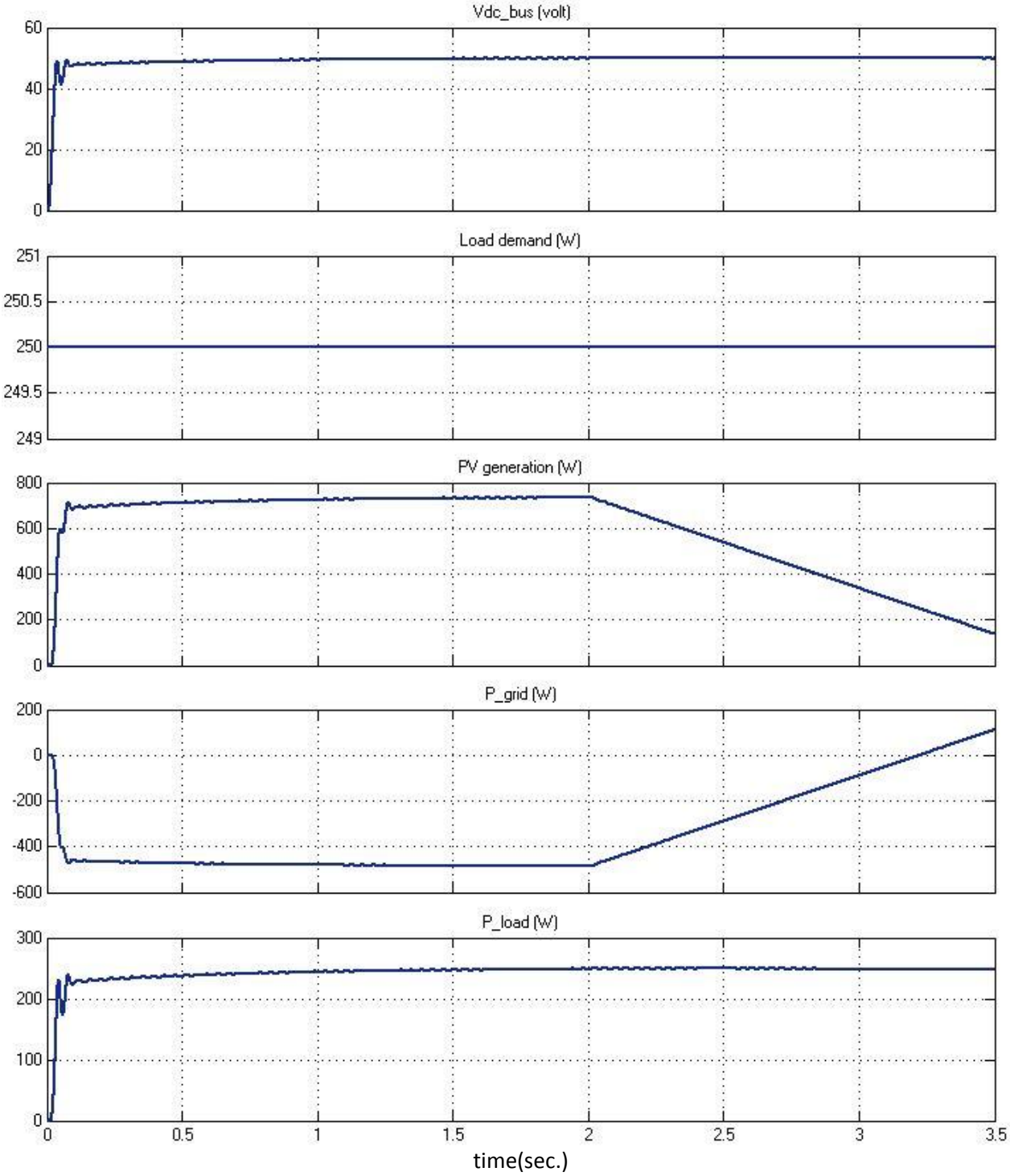

Figure 4.12: Simulation results for power flow in DC microgrid operation considering the variation in power generation from PV module.

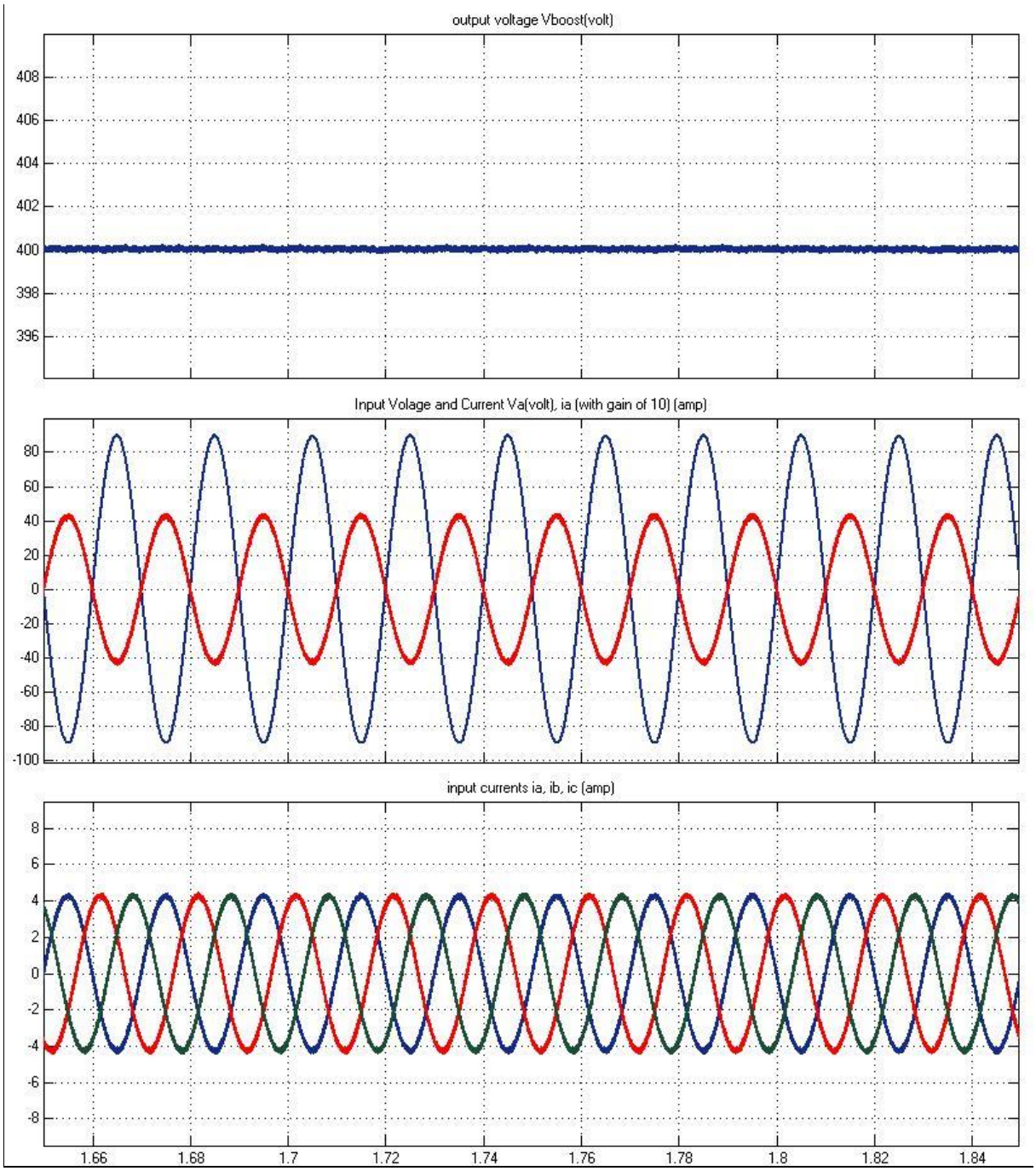

Figure 4.13: Simulation results of output boost voltage and ac side waveforms in inversion mode operation of PFC circuit

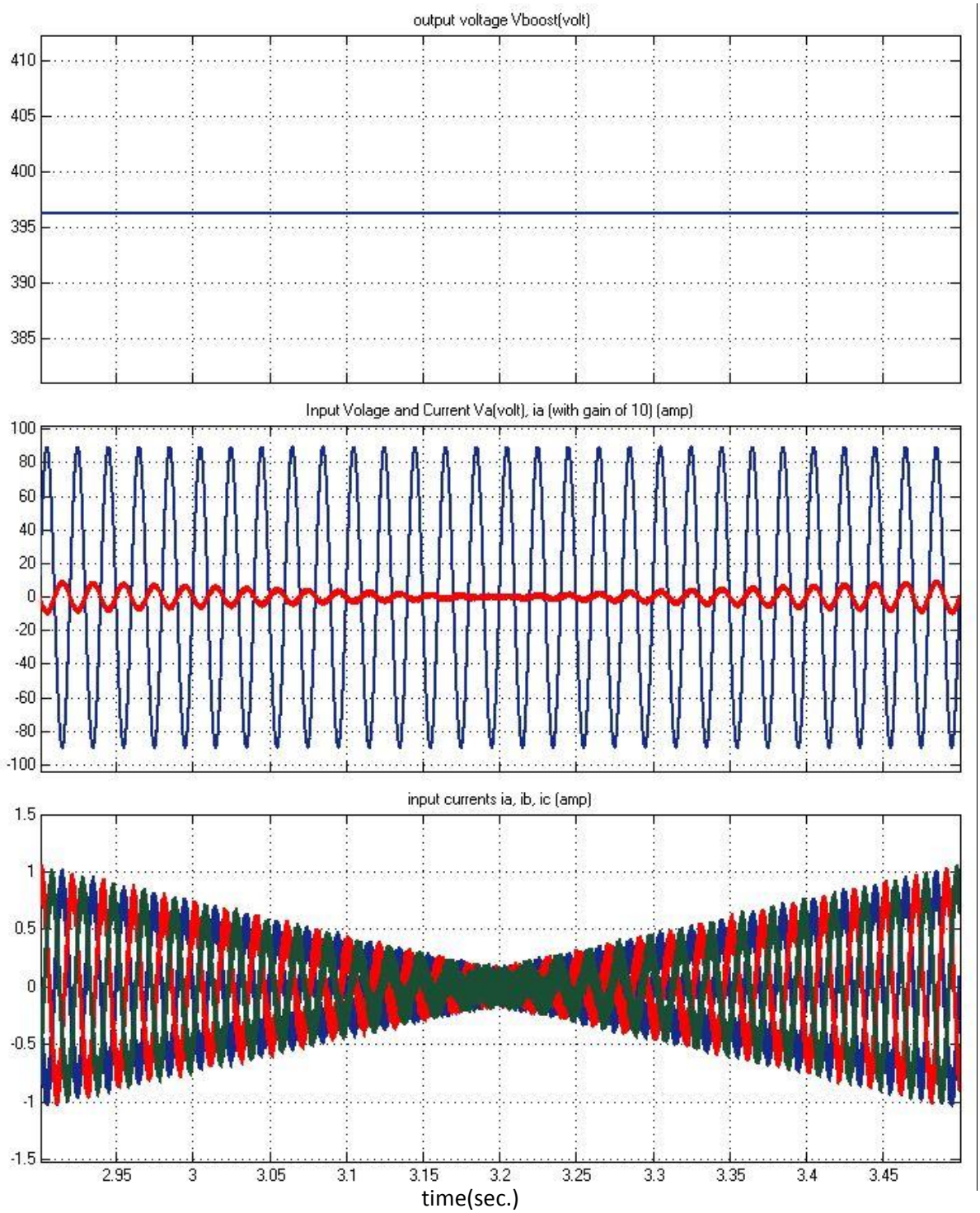

Figure 4.14: Simulation results of output boost voltage and ac side waveforms during transition from inversion to rectification mode operation of PFC circuit.

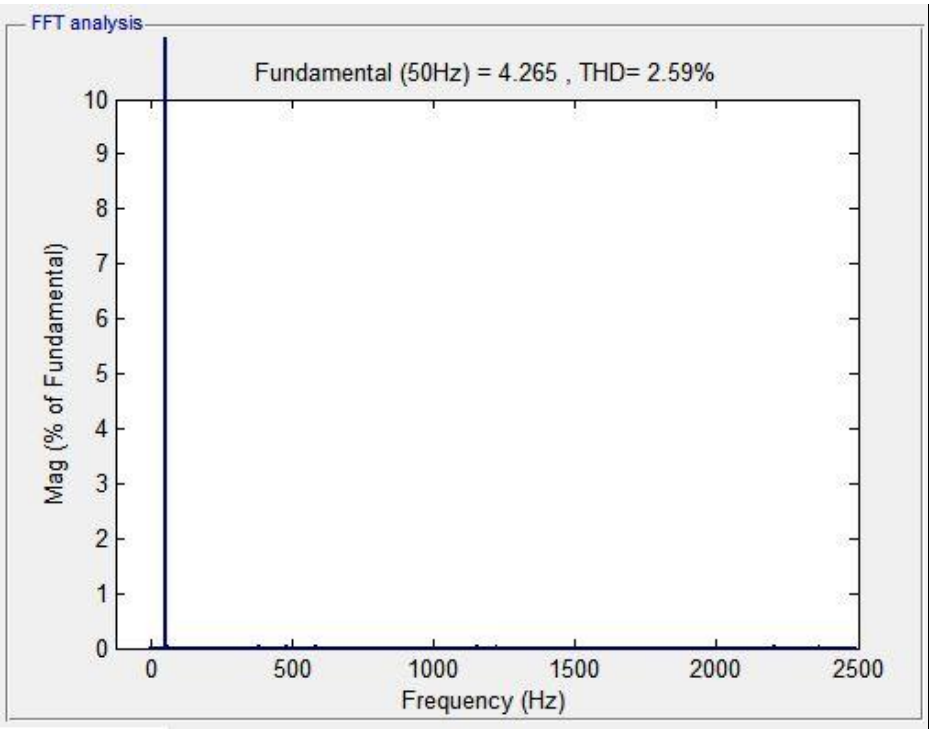

Figure 4.15: FFT analysis of ac side i_a during inversion mode operation of PFC circuit.

The MATLAB Simulink model of the system was tested successfully for the conditions of load variation and variation in irradiance. MPPT control with boost converter on PV system was able to extract maximum power for a given condition. The Six-switch two-level three phase boost rectifier managed unity power factor in the AC side. The difference between power generated by PV system and power requirement of load was compensated by control of bi-directional dc-dc converter with maintaining DC bus voltage constant.

CHAPTER 5: HARDWARE DEVELOPMENT

5.1 Development of MOSFET switch driver circuit

A single MOSFET switch driver circuit contains all the 3 circuits(power supply +12V,snubber circuit, amplification & isolation circuit). The pulse amplification circuit for MOSFT is shown Figure 6.4. The opto-coupler MCT-2E provides necessary isolation between the low voltage isolation circuit and high voltage power circuit. The pulse amplification is provided by the output amplifier transistor 2N222. When the input gating signal is +5V level, the input transistor saturates, the LED of opto-coupler conducts and the light emitted by it falls on the base of the phototransistor, thus forming the base drive. The output transistor thus receives no base drive and remains in the cut-off state and a +12V pulse (amplified) appears at its collector terminal. The +12V needed by firing circuit is locally generated ate each switch using a 220/18V transformer and 7812 regulated IC along with a rectification circuit and capacitors. When the input gating signal reaches ground level, the input switching transistor goes to cut off state and opto-coupler LED remains off, thus emits no light and therefore the photo transistor remains off. The output transistor receives base drive and saturates, hence the output falls to zero level. Therefore, the circuit provides proper amplification and isolation. Further, since slightest spike above 20V can damage the MOSFET, a 12V Zener diode is connected across the output isolation circuit. This clamps the triggering voltage to 12V.

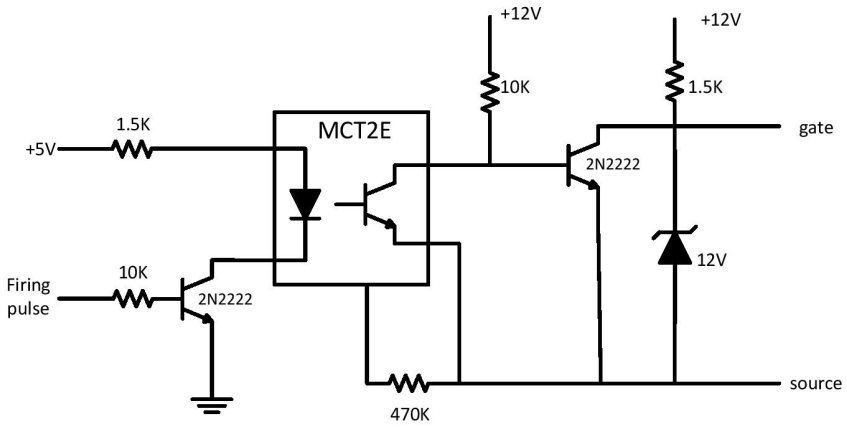

Figure 5.1: Pulse amplification circuit for MOSFET

Switching high current in a very short interval of time gives rise to voltage transients that could exceeds the rating of the MOSFET. The rated Gate-to-Source voltage of MOSFET is 20V. Snubbers are therefore needed to protect the switch from transients. Snubber circuit for MOSFET is shown in Figure 6.5. The diode prevents the discharging of the capacitor via the switching device, which could damage the device because of large discharge current. An additional protective Metal Oxide Varistor (MOV) is used across each device to protect against over voltage across the device.

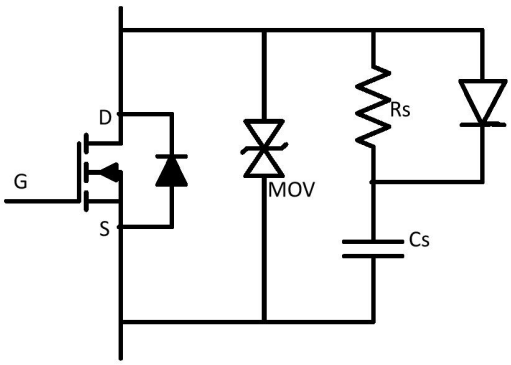

Figure 5.2: Snubber Circuit for MOSFET

5.2 Development of Measuring Circuit

5.2.1 Current Sensing Circuit

For measuring either the Source currents, load currents and compensator currents the Hall Effect current sensors (HTP 25) are used. The circuit diagram of the Hall Effect current sensor along with a buffer and a scalar circuit is shown in Fig 5.3. Here a current of I (A) in power network is converted into ± 5V range. These current sensors provide galvanic isolation between high voltage power circuit and the low voltage control circuit and require a nominal supply voltage of the ±12V to ±15V. For a chosen primary turns (N_P), the conversion ratio (cr_i) of current sensor, which is 1000:1, and the output resistance of the current sensor is taken as 100 Ω. The voltage input to the buffer circuit is calculated by the equation.

$$v_{0i} = R_0\left(\frac{N_p i}{cr_i}\right) \qquad (10)$$

Thus the voltage v_{0i} is scaled properly with the scalar circuit. The output voltage can be given to the controller kit with the help of ADC.

Each Current sensor (TELCON) circuit

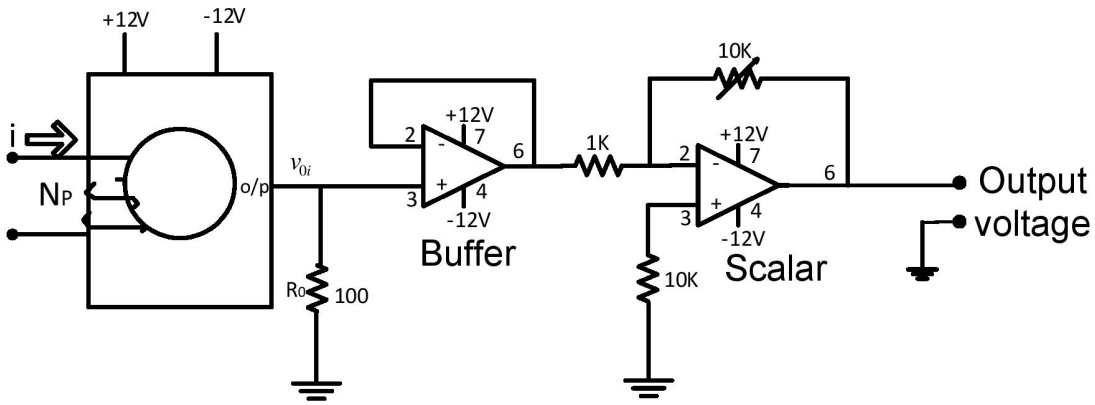

Figure 5.3: Current sensor circuit

5.2.2 Voltage Sensing Circuit

AC source voltages v_{sa},v_{sb} and v_{sc}(phase to neutral) are given as the inputs for PLL. The DC capacitor voltages are also required to be sensed. Only sensing two phase voltages are sufficient for three phase three wire system. The circuit diagram of the sensing voltage along with the buffer and scalar circuit is shown in the figure 5.4. The AD202JN is an isolation amplifier in the present experimental setup the power circuit voltage which is in the range of ±500 V is converted into ±5V range. The voltage at the output of the isolation amplifier is $v_{ov} = v_1\left(\frac{R_2}{R_1 + R_2}\right)$. Thus the output voltage v_{ov} is properly scaled by a scalar circuit and the output voltage can be given to the ADC of controller kit.

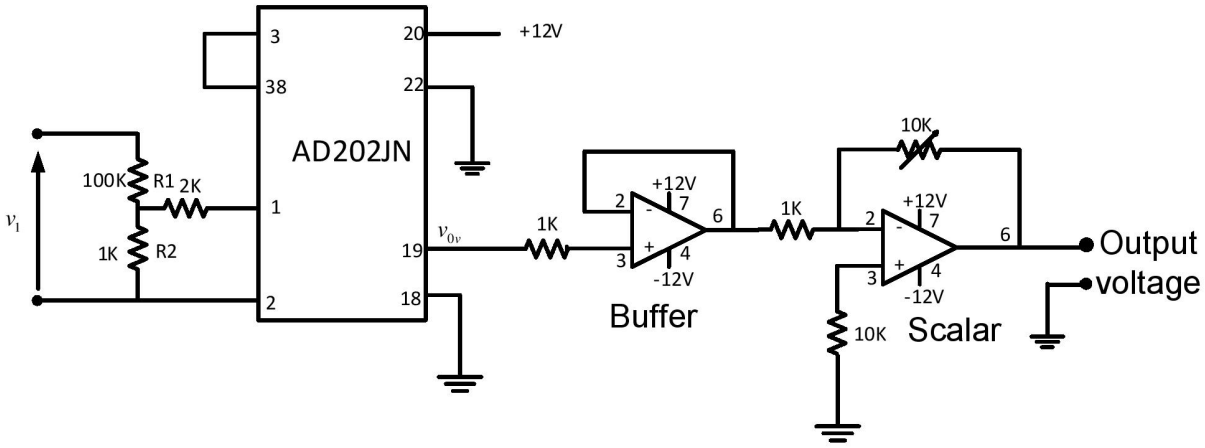

Figure 5.4: Voltage sensing circuit

5.2 Development of Regulated Power Supplies

DC regulated supplies (+12V GND -12V, +5V) are required for providing biasing to various circuits like pulse amplification and isolation circuits, hysteresis controller and voltage detectors etc. using IC's 7812 for +12V, IC 7912 for -12V and 7805 for +5 V The circuit diagram of the power supplies is as shown in following figures. A single +5V power supply is required for all the switches

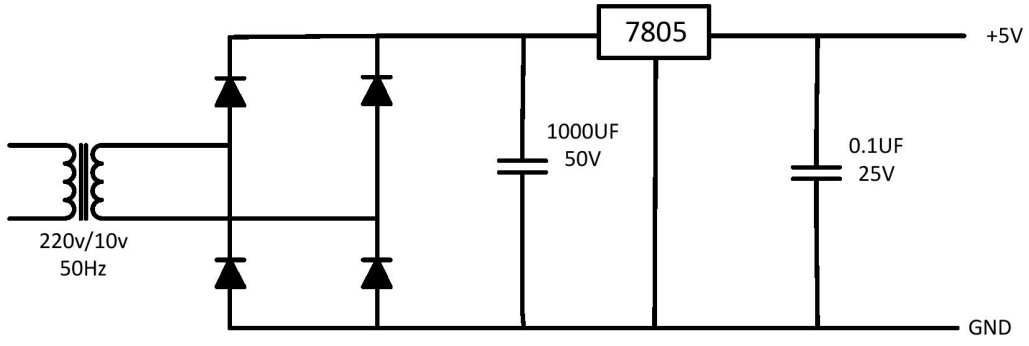

(a)

A single +12 0 -12V power supply is required for current sensor and voltage sensor circuit

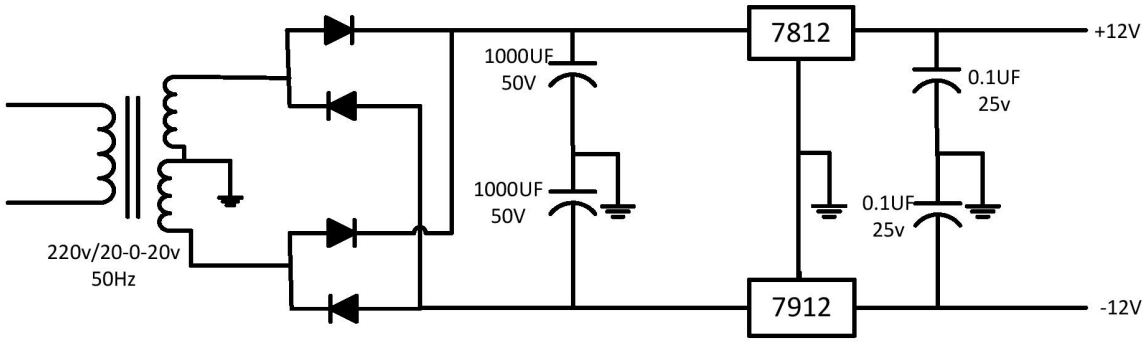

(b)

Figure 5.5: Connection diagram for power supplies (a).+5V (b).-12V,0,+12V

CHAPTER 6: CONCLUSIONS

The project was aimed at development of three phase universal PFC circuit for DC microgrid application. A three phase six switch boost rectifier and a bidirectional buck boost converter were used in two stage conversion technique with the capability of bidirectional power processing as well as unity power factor operation with nearly sinusoidal ac current. Hysteresis band current control and triangular carrier wave PWM control were used in bidirectional boost rectifier. Maximum power point tracking through P&O method on boost converter was implemented for photovoltaic system. This MPPT algorithm was used in DC microgrid operation to extract maximum power from PV module. The two stage PFC circuit was successfully investigated for power management in different DC microgrid operation circumstances.

PHOTOGRAPHS OF HARDWARE DEVELOPED

MOSFET SWITCHES

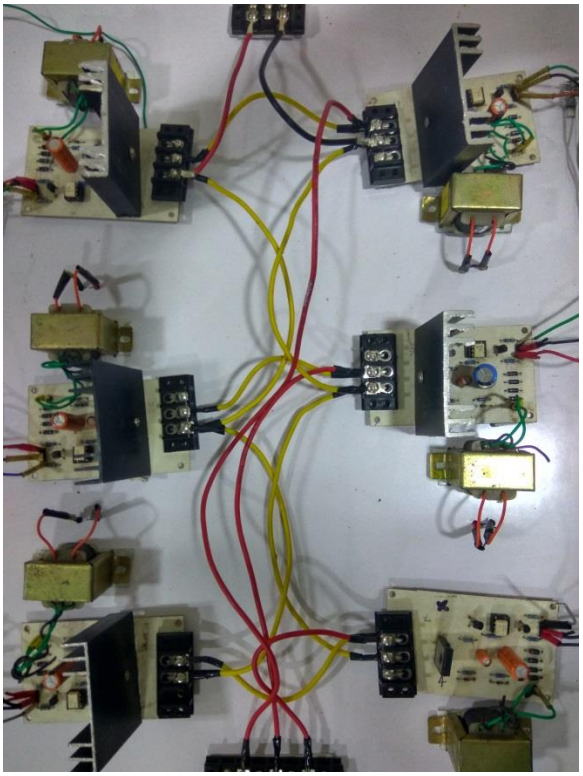

REGULATED POWER SUPPLY

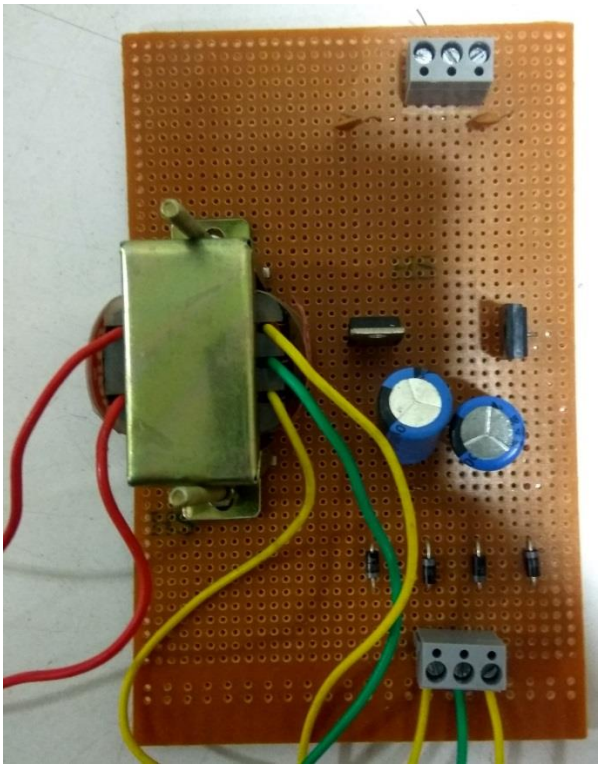

VOLTAGE SENSOR CIRCUIT

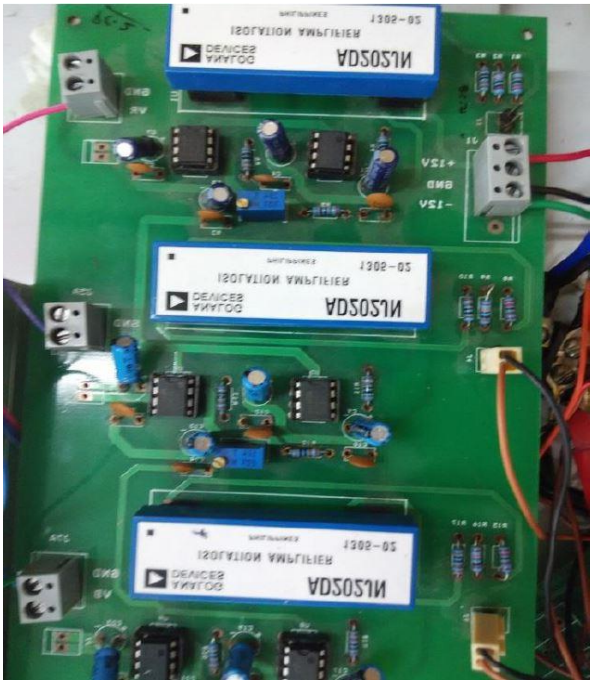

CURRENT SENSOR CIRCUIT

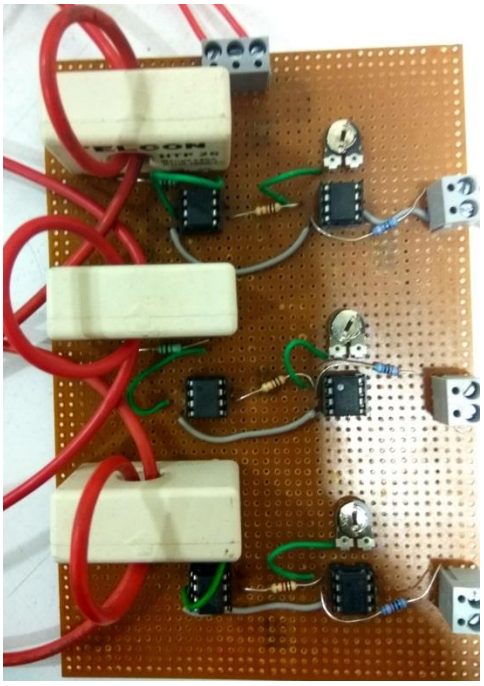

References

[1] J.Lee; B.Han; “Operational Characteristic Analysis of DC Micro-grid using Detailed Model of Distributed Generation” *IEEE PES T & D*, PP:1-8; 2010

[2] Ching-Chih Huang; Min-Jui Chen; Yung-Tang Liao, Chan-Nan Lu; ”DC Microgrid Operation Planning” *Renewable energy research and application*; pp: 1-7, 2012

[3] IEEE Standard 519-1992, *IEEE Recommended Practices and Requirements for Harmonic Control in Electrical Power Systems*

[4] E. Wernekinck, A. Kawamura and R. Hoft, "A high frequency AC/DC converter with unity power factor and minimum harmonic distortion," in *IEEE Transactions on Power Electronics*, vol. 6, no. 3, pp. 364-370, Jul 1991.

[5] J. W. Dixon, "Feedback control strategies for boost type PWM rectifiers," Colloquium in South America, 1990., Proceedings of the 1990 IEEE, Argentina, Brazil, Chile, 1990, pp. 193-198.

[6] R. Wu, S. B. Dewan and G. R. Slemon, "Analysis of an AC to DC voltage source converter using PWM with phase and amplitude control," *Industry Applications Society Annual Meeting, 1989., Conference Record of the 1989 IEEE*, San Diego, CA, USA, 1989, pp. 1156-1163 vol.1.

[7] M. P. Kazmierkowski and L. Malesani, "Current control techniques for three-phase voltage-source PWM converters: a survey," in *IEEE Transactions on Industrial Electronics*, vol. 45, no. 5, pp. 691-703, Oct 1998.

[8] J. Kikuchi and T. A. Lipo, "Three-phase PWM boost-buck rectifiers with power-regenerating capability," in *IEEE Transactions on Industry Applications*, vol. 38, no. 5, pp. 1361-1369, Sep/Oct 2002.

[9] R. H. Lasseter and P. Paigi, "Microgrid: a conceptual solution," *Power Electronics Specialists Conference, 2004. PESC 04. 2004 IEEE 35th Annual*, 2004, pp. 4285-4290 Vol.6.

[10] B. Wang, M. Sechilariu and F. Locment, "Intelligent DC Microgrid With Smart Grid Communications: Control Strategy Consideration and Design," in *IEEE Transactions on Smart Grid*, vol. 3, no. 4, pp. 2148-2156, Dec. 2012.

[11] M. Liserre, A. Dell'Aquila and F. Blaabjerg, "Design and control of a three-phase active rectifier under non-ideal operating conditions," *Industry Applications Conference, 2002. 37th IAS Annual Meeting. Conference Record of the*, Pittsburgh, PA, USA, 2002, pp. 1181-1188 vol.2.

[12] Jung-Hyo Lee, Jung-Song Moon, Yong-Seok Lee, Young-Real Kim and Chung-Yuen Won, "Fast charging technique for EV battery charger using three-phase AC-DC boost converter," *IECON 2011 - 37th Annual Conference on IEEE Industrial Electronics Society*, Melbourne, VIC, 2011, pp. 4577-4582.

[13] Williams K. Francis; Prof. Shanifa Beevi S; Prof. Johnson Mathew;" MATLAB/Simulink PV Module Model of P&O And DC Link CDC MPPT Algorithms with Labview Real Time Monitoring And Control Over P&O Technique" *IJAREEIE* Vol. 3, Special Issue 5, December 2014

[14] Vijayakumar.R; M.P. Mohandass; D.Rajasindhu; S.Angeline Sreeja;"Standalone Operation of PMSG based Wind Turbine Generating Systems with Energy Management by Hybrid Energy Storage" *IJAREEIE* Vol. 3, Special Issue 5, December 2014

[15] J. Lee and B. Han, "Operational characteristic analysis of DC micro-grid using detailed model of distributed generation," *IEEE PES T&D 2010*, New Orleans, LA, USA, 2010, pp. 1-8.